EXPERIMENTAL TREATMENT OF BURN VICTIMS IN FIELD HOSPITALS

FINAL REPORT

IOANNIS V. YANNAS

AUGUST 28, 1992

Supported by

U.S. ARMY MEDICAL RESEARCH AND DEVELOPMENT COMMAND
Fort Detrick, Frederick, Maryland 21702-5012

Contract No. DAMD17-87-C-7130

Massachusetts Institute of Technology
77 Massachusetts Avenue
Cambridge, Massachusetts 02139-4309

DISCLAIMER NOTICE

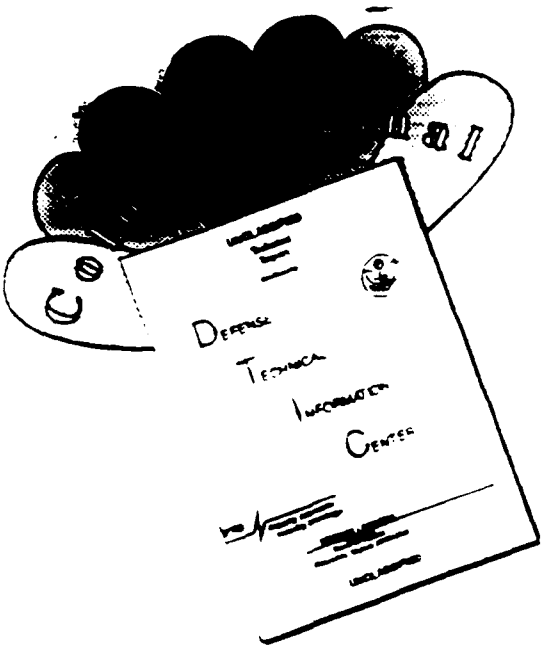

THIS DOCUMENT IS BEST QUALITY AVAILABLE. THE COPY FURNISHED TO DTIC CONTAINED A SIGNIFICANT NUMBER OF COLOR PAGES WHICH DO NOT REPRODUCE LEGIBLY ON BLACK AND WHITE MICROFICHE.

REPORT DOCUMENTATION PAGE

Form Approved
OMB No 0704-0188

1. AGENCY USE ONLY (Leave blank)	2. REPORT DATE	3. REPORT TYPE AND DATES COVERED
	August 28, 1992	Final 30 Sep 87 - 29 Nov 91

4. TITLE AND SUBTITLE
Experimental Treatment of Burn Victims in Field Hospitals

5. FUNDING NUMBERS
DAMD17-87-C-7130

63002A
3M263002D840 DA
DA313303

6. AUTHOR(S)
Ioannis V. Yannas

7. PERFORMING ORGANIZATION NAME(S) AND ADDRESS(ES)
Massachusetts Institute of Technology
77 Massachusetts Avenue
Cambridge, Massachusetts 02139-4309

8. PERFORMING ORGANIZATION REPORT NUMBER

9. SPONSORING / MONITORING AGENCY NAME(S) AND ADDRESS(ES)
U.S. Army Medical Research & Development Command
Fort Detrick
Frederick, Maryland 21702-5012

10. SPONSORING / MONITORING AGENCY REPORT NUMBER

11. SUPPLEMENTARY NOTES

12a. DISTRIBUTION / AVAILABILITY STATEMENT
Approved for public release;
distribution unlimited

12b. DISTRIBUTION CODE

13. ABSTRACT *(Maximum 200 words)*

The research effort centered on the development of an experimental treatment of burn victims. The specific objective was the development of an immediately graftable, nonimmunogenic material which supplies the function both of the dermis and the epidermis over an indefinite period. The objective was largely accomplished in the guinea pig model. The successful design was based on a biologically specific analog of extracellular matrix (ECM) which was seeded with foreign epidermal cells. A demonstrated rejection model was used together with a staining technique for identification of cells involved in graft rejection. The transplantation of epidermal cells using the ECM analog showed no evidence of rejection in 12 out of 14 grafts. Long term observations showed gross and histologic evidence of synthesis of new physiologic dermis and epidermis (no hair follicles). It is suggested that these grafts can be used to avoid problems of autologous tissue availability.

14. SUBJECT TERMS
Burns; Skin grafting; Immunology; Trauma;
Skin regeneration; RA 2

15. NUMBER OF PAGES

16. PRICE CODE

17. SECURITY CLASSIFICATION OF REPORT	18. SECURITY CLASSIFICATION OF THIS PAGE	19. SECURITY CLASSIFICATION OF ABSTRACT	20. LIMITATION OF ABSTRAC
Unclassified	Unclassified	Unclassified	Unlimited

FOREWORD

Opinions, interpretations, conclusions and recommendations are those of the author and are not necessarily endorsed by the U.S. Army.

_____ Where copyrighted material is quoted, permission has been obtained to use such material.

_____ Where material from documents designated for limited distribution is quoted, permission has been obtained to use the material.

_____ Citations of commercial organizations and trade names in this report do not constitute an official Department of the Army endorsement or approval of the products or services of these organizations.

__✓__ In conducting research using animals, the investigator(s) adhered to the "Guide for the Care and Use of Laboratory Animals," prepared by the Committee on Care and Use of Laboratory Animals of the Institute of Laboratory Animal Resources, National Research Council (NIH Publication No. 86-23, Revised 1985).

_____ For the protection of human subjects, the investigator(s) have adhered to policies of applicable Federal Law 45CFR46.

_____ In conducting research utilizing recombinant DNA technology, the investigator(s) adhered to current guidelines promulgated by the National Institutes of Health.

PI Signature _____ Date 8/24/92

Table of Contents

Introduction

Background and Summary of Results

This is the final report covering the entire period for contract No. DAMD17-87-C-7130.

The research effort centered on the development of an experimental treatment of burn victims. The specific objective was the development of an immediately graftable, nonimmunogenic material which supplies the function both of the dermis and the epidermis over an indefinite period. The method used to supply the missing organ was regeneration, by use of cell-seeded analogs of extracellular matrix (ECM).

The background of this study is a novel surgical treatment which induces regeneration of nearly physiologic dermis in patients with loss of skin over the entire thickness. This treatment was developed in studies at MIT starting in 1974. Since the epidermis was not regenerated, the treatment was later completed by a second procedure in which the regenerated dermis was covered definitively with a thin autoepidermal graft. This early treatment was based on the use of analogs of the extracellular matrix (ECM) which were synthesized using standard procedures of biochemistry and polymer chemisty. One of these analogs, a highly porous collagen-glycosaminoglycan (CG) copolymer has been tested on over 100 massively burned patients in the context of a randomized clinical trial involving 11 clinical centers. Reports of the surgical, histologic and immunologic results of this clinical trial have been independently published recently.

A single surgical procedure for the regeneration of both a dermis and an epidermis was developed after further studies with animals at MIT during 1980–84. In this modified treatment the ECM analog was first seeded with autologous (host) uncultured epidermal cells from a biopsy prior to grafting the full-thickness skin wound. A neoepidermis reached confluence over the entire wound area (up to 16 cm^2) in 2 weeks while a nearly physiologic dermis was synthesized underneath.

During the contract period (1987–91) the effort was focused on development of a surgical procedure which would induce regeneration both of the dermis and the epidermis using a single treatment that would provide certain clear advantages over previous designs. The advantages sought were:

(a) improved understanding of the cell-biological and molecular-biological mechanisms of skin regeneration in the presence of the cell-seeded ECM analog, leading to improved control of the parameters of the procedure and demonstrating a surgical protocol of improved reliability (see Sections 1–3 of this report),

(b) development of a quantitative assay to evaluate the relative merit of various ECM analogs in improving the architecture of collagen fibers in the regenerated dermis, thereby leading to a more nearly physiologic dermis and to a higher long-term benefit for the patient (Section 4), and,

(c) replacement of host seeded cells with foreign seeded cells, leading to a more versatile treatment for the severely burned patient (Sections 5-7).

Studies of the mechanistic aspects of dermal regeneration revealed a persistent relation between the ability of an ECM analog to delay the onset of wound contraction significantly and its ability to induce regeneration of nearly physiologic dermis (rather than lead to formation

of scar). Systematic variation in the structure and composition of the ECM analogs using procedures of polymer chemistry and biochemistry showed that delay of the onset of contraction by as much as 10 days was observed when the physical and chemical structure of the ECM analog was controlled within limits which were unexpectedly narrow and which were identified. Partly regenerated skin was remarkably similar to normal guinea pig skin in most respects and was significantly different than scar. The new skin totally lacked hair follicles and skin adenexa (see **Section 1**).

The surprising paucity of ECM structures which induced regeneration suggested strongly the presence of a highly specific interaction between the ECM analog and the mesenchymal cells migrating into it. Ultrastructural studies of interactions between the seeded cells and the ECM analog in the woundbed up to Day 21 following grafting identified highly organized associations between rows of mononuclear cells and CG fibers which also involved prominenet extension of filopodia toward the CG fiber surface. The quality of skin regenerated by use of (host) cell-seeded ECM analogs was also studied ultrastructurally. One year following grafting the graft sites ultrastructurally resembled normal dermis, with well-defined papillae, normal anastomosing superficial vasculature and nerve fibers (see **Section 2**).

In a companion study by light microscopy contractile cells from the ungrafted and grafted wound beds were immunohistochemically stained using a monoclonal mouse antibody against α-smooth muscle actin. The results of the light microscopic study showed that ECM analogs disoriented the long axes of contractile cells in the woundbed and also interfered with formation of an uninterrupted network of contractile cells. These findings suggested that ECM analogs delay contraction by interfering with the process of scale-up of mechanical force from cell to organ but did not provide information on the molecular mechanism of the interaction between cell and ECM analog. Continuation of this study should provide new information on the cell-biological mechanism of wound contraction in mammals. This study is also continuing in the direction of identifying the fibroblast surface receptors which mediate contraction in the absence of ECM analogs. It is also leading to a comparison of the distribution of fibronectin receptors and collagen receptors before and after onset of contraction in the presence of ECM analogs and controls (see **Section 3**).

A new quantitative procedure was developed which reports the average orientation and diameter of collagen fibers in histological sections of dermis, regenerated dermis and scar. The procedure is based on analysis of the scattering patterns obtained by transmittimg laser light through conventional histologic sections of tissue. Light scattering measurements were independent of the nature of histological stain. Collagen fibers in sections of regenerated dermis had values of average orientation and diameter which were intermediate between those of intact, mature dermis and those of scar (see **Section 4**).

A method for separating the Langerhans cell population from a mixed dermal and epidermal cell population was studied in a preliminary way. The objective was preparation of skin grafts which are donor-independent. This research was based on the hypothesis that Langerhans cells in the skin are the most significant contributors to rejection of skin grafts. Several methods were experimentally tested before designing a monolayer panning technique. The panning technique was based on the use of a monoclonal antibody with highly specific affinity. Individual steps of the panning technique was based on use of OKT-6 antibody which is known to recognize the CD1a antigen in humans. However, the efficacy of the method was not conclusively tested with the guinea pig model due to eventual lack of evidence that the antibody used recognized a similar antigen in guinea pig cells (see **Section 5**).

Cryopreservation of epidermal cells (guinea pig) was demonstrated at −80°C after 3 days of freezing. This result extended our previous development of a cryopreservation method for epidermal cells −196°C. Cryoprotection with dimethylsulfoxide at −80°C yielded higher cell viability (90%) than with glycerol (60%). Cryopreservation at −80°C (dry ice temperature) is proposed as a relatively convenient method of storing epidermal cells prior to seeding in ECM analogs for the preparation of skin grafts (see **Section 6**).

An ECM analog was used as a carrier of foreign epidermal cells in trasplantation experiments with guinea pigs. Using a demonstrated rejection model and staining technique, cells involved in graft rejection were identified. Transplantation of epidermal cells seeded in an ECM analog produced a significantly ($p = 0.05$) lower response than transplantation of whole skin. The transplantation of epidermal cells using the ECM analog showed no evidence of rejection in 12 out of 14 grafts. In addition, long term (102 days) observations with the same model (foreign cells in an ECM analog) showed gross and histologic evidence of synthesis of new dermis and epidermis. These results suggest a potential clinical use for ECM analogs seeded with foreign cells. Use of such grafts could avoid problems of autologous tissue availability and should be studied further (see **Section 7**).

Experimental Methods/Results

1 Partial Regeneration of Adult Mammalian Skin Induced by an Analog of Extracellular Matrix

I.V. Yannas, D.P. Orgill, Elaine Lee, Ariel Ferdman and George F. Murphy

1.1 Abstract

Certain highly porous, crosslinked collagen-glycosaminoglycan copolymers have induced partial morphogenesis of skin when seeded with dermal and epidermal cells and then grafted on standard, full-thickness skin wounds in the adult guinea pig. A mature epidermis and a nearly physiological dermis, which lacked hair follicles but was demonstrably different from scar, were regenerated over areas as large as 16 cm^2. These chemical analogs of extracellular matrices (ECMs) were morphogenetically active provided that the average pore diameter ranged between 20 and 125 μm, the resistance to degradation by collagenase exceeded a critical limit which was determined empirically, and the density of autologous dermal and epidermal cells inoculated therein was higher than 5×10^4 per cm^2 wound area. Unseeded copolymers with physical structures which were within these limits delayed the onset of wound contraction by about 10 days but did not eventually prevent it. Seeded copolymers not only delayed contraction but eventually arrested and reversed it while new skin was being regenerated. Regeneration of the dermis does not occur spontaneously in the adult mammal. The epidermis is regenerated spontaneously provided there is a dermal substrate over which it can migrate. The data identify a model ECM which acts as if it were an insoluble growth factor with narrowly specified physicochemical structure, perhaps functioning as a transient basal lamina during morphogenesis of skin.

1.2 Introduction

Extracellular matrices (ECMs) are continuously being remodeled during development, i.e., synthesized, degraded, and resynthesized [1–5]. Healing of a deep skin wound also requires remodeling of an ECM, the basal lamina (basement membrane) between the epidermis and the dermis [2]. ECMs are largely insoluble and non-diffusible, and they confer stiffness and strength to multicellular systems [1,2]. During remodeling the ECM necessarily suffers degradation of macromolecular chains, a process which dramatically reduces the insolubility of ECM and impairs its role as mechanical reinforcement of a multicellular system undergoing development. It is not clear just how the resistance of the ECM to degradation affects its role during morphogenesis.

In physical terms, ECMs can be described as macromolecular networks which are covalently crosslinked and are highly swollen in extracellular fluid. Accordingly, the physical structure of an ECM can initially be characterized by specifying the volume fraction of macromolecular components (swelling ratio), the average diameter of pores in the highly swollen network, the density of crosslinks tying chains to each other, and the degree of crystallinity present. This model leads to questions such as: Is it necessary for a developmentally active ECM to persist as an undegraded, crosslinked macromolecular network (and, therefore, remain insoluble and non-diffusible) over a critical timescale? Is it necessary for such an ECM to contain pores

of a critical size? We have answered these questions in a preliminary way by use of well-defined collagen-glycosaminoglycan (CG) graft copolymers which are simple chemical analogs of ECM. A series of CG copolymers was prepared in a way that morphogenetic effects due to the degradation rate of the copolymers in collagenase could be studied in isolation from effects due to their average pore diameter. Other structural features, including the swelling ratio, the degree of crystallinity and the chemical composition, were not changed through the current series of copolymers, and the potential morphogenetic effects of these other parameters are the subject of ongoing study.

The chemical analogs of ECM were fabricated into membranes and used to study skin morphogenesis in the standard wound healing model of Billingham and Medawar [6,7]. In this model the complete dermis and epidermis are excised over a rectangular area from the back of a rodent, and the striated muscle underneath is thereby exposed, serving as a reproducible wound bed. When left ungrafted this wound bed contracts at a well-known rate until opposite wound edges touch and a linear scar is formed. Dermis is not regenerated in the ungrafted Billingham-Medawar skin wound model [6,7]. It has been shown that a membrane fabricated from at least one member of the CG copolymer series, which was relatively resistant to collagenase [8] and was highly porous [9], delayed significantly the onset of wound contraction when grafted on this animal model [9]. Furthermore, when seeded with autologous dermal and epidermal cells, this CG membrane graft induced partial regeneration of the dermis in the same model [10,11]. In the current study we found that there were severe restrictions to the physical structure of cell-seeded CG copolymers which induced morphogenesis. Only copolymers with critically adjusted pore size and degradation rate delayed the kinetics of wound contraction remarkably before undergoing degradation. When seeded with a minimal density of autologous epidermal and dermal cells, members of this group of contraction-inhibiting copolymers were capable of arresting contraction and inducing synthesis of a dermis and an epidermis over the area of the wound. The data support the conclusion that these cell-seeded, simple chemical analogs of ECM induced morphogenesis of skin provided that their macromolecular network structure was adjusted within highly specific limits.

1.3 Materials and Methods

1.3.1 Synthesis of CG copolymers

A white coprecipitate of type I collagen from bovine hide and of chondroitin 6-sulfate from shark cartilage in 0.05M acetic acid, pH 3.2, was converted into a highly porous, white membrane with a fractional pore volume of ca. 0.99 by freeze-drying, as described elsewhere in detail [8,12,13]. Control of the average pore diameter was achieved by adjusting the initial shelf temperature in the range $-90°$ to $-5°C$, respectively [13]. Subsequent exposure of the dry solid to 105°C and a vacuum of 50 torr over 24 h introduced covalent crosslinks between the polypeptide chains of collagen without denaturing it to gelatin [9,14,15]. The porous collagen-glycosaminoglycan (CG) sheet was knife-coated with a thin layer of viscous poly(dimethyl siloxane) prepolymer (PDMS, Silastic Medical A, Dow Corning, Midland, MI) to control the loss of moisture from the wound bed as well as to prevent bacterial contamination. Following polymerization of the PDMS to a 0.025-mm-thick elastomeric layer, the bilayer membrane was immersed in a bath containing 0.25% w/w aqueous glutaraldehyde in 0.05M acetic acid and the collagenous component of the CG copolymer underwent therein additional covalent crosslinking [12]. Increase of the residence time in the glutaraldehyde bath from 0 to 24 h

yielded CG copolymers varying widely in their crosslink density, as reflected in values of $\overline{M_c}$, the average molecular weight between crosslinks [12], which ranged from ca. 60 kD to ca. 12 kD, respectively. It has been shown that the degradation rate of CG copolymers which are either implanted subcutaneously in rodents [9] or exposed to collagenase *in vitro* [16] increases as $\overline{M_c}$ increases [9]. Following rinsing in deionized water over 24 h the glutaraldehyde concentration in the rinse water was found to be less than 5 ppm using the analytical reagent 4-amino-3-1-hydrazino-5-1-mercapto-1,2,4-triazole (Purpald, Aldrich, Milwaukee, WI) [17]. No histological or other evidence of toxicity due to exposure of the CG copolymers to glutaraldehyde during preparation was detected over several years of their use as grafts or implants in animals and humans [9,10,11]. Sterile procedures were followed in preparation of membranes.

1.3.2 Physicochemical characterization of CG copolymers

The average pore diameter was determined either with a scanning electron microscope [13] or by embedding the porous membrane in methyl methacrylate, sectioning, staining with toluidine blue and viewing with an image analyzer. The glycosaminoglycan content was determined by hexosamine assay [12] and averaged $2.6 \pm 0.3\%$ (w/w; dry basis) through the copolymer series. Small-angle x-ray scattering studies showed that the collagen fibers became highly swollen and disaggregated, and lost their banding below pH 4.25 ± 0.30 [18]. Exposure to glutaraldehyde before final rinsing and buffering to pH 7 prevented the recovery of the banding pattern prior to grafting [18]. Nevertheless, infrared spectroscopic measurements [19] showed that the triple helical structure of collagen was intact at the time of grafting. The degradation rate of CG copolymers in collagenase was determined by a colorimetric procedure following incubation of the finely comminuted polymer for 5 h at 37°C in a stirred 0.08 % w/v solution of bacterial collagenase from *Clostridium histolyticum* (GIBCO, Grand Island, NY) in a buffer, pH 7.4 [20]. Previous studies have shown that the use of bacterial collagenase as an *in vitro* empirical screening device provides an order ranking of collagen implants according to degradation rate which agrees with *in vivo* observations [9,16]. Assay results were expressed in enzyme units which were calculated using a standard solution of 0.002M L-leucine. By definition, one enzyme unit liberates amino acids from collagen which are equivalent in ninhydrin color to 1.0 μmole of L-leucine in 5 h at pH 7.4 and at 37°C [20].

1.3.3 Cell-seeding procedures

CG copolymers were seeded with autologous, uncultured, dermal and epidermal cell suspensions which were enriched in basal cells [10]. The procedure used for cell extraction depends on careful control of the standard trypsinization procedure of Medawar [21], as elaborated by Prunieras and coworkers [22,23], who reported a basal cell content of $71 \pm 4\%$ for these cell preparations. In our work a 0.2-mm-thick layer of skin was harvested from the guinea pig dorsum by use of a dermatome and at least 10×10^6 viable cells per cm^2 of biopsy were obtained. The desired density of cells inside the copolymer layer was arrived at by centrifugation. Seeding was accomplished by equilibrating cell-free CG membranes, with silicone layer attached, for 30 min in DMEM medium enriched with 10% fetal bovine serum (Hazelton Research, Lenexa, KS) and then placing the membranes in a polycarbonate holder specially designed to maintain the centrifugal force vector perpendicular to the plane of the membrane. The cell suspension was pipetted on top of the porous CG copolymer layer and centrifuged for 15 min at 100g. Scanning electron microscopy of the seeded membrane showed that the majority of cells had

been positioned near the interface between the silicone layer and the CG layer.

1.3.4 Surgical procedures

White female adult Hartley guinea pigs weighing about 400 ± 50 g were grafted and bandaged as described elsewhere in detail [9]. The excision protocol used followed closely the standard mammalian free skin grafting model described by Billingham and Medawar [6,7]. The skin was excised down to, but not including, the *panniculus carnosus*, the layer of muscle responsible for skin-twitching movements in rodents. An anatomically well-defined wound bed, usually measuring 1.5 cm by 3.0 cm but as high as 4.0 cm by 4.0 cm in some animals, was thereby prepared. The test group of animals was grafted with a CG copolymer membrane coated with PDMS. Control wounds were treated only with a Xeroform gauze (ungrafted) or were autografted [6,7]. The wound area was calculated from photographs using measurements taken from edges of cut dermis and not from the advancing edge of epithelial cell sheets, as described previously [6,7,9]. From these data we estimated the wound half life, $t_{1/2}$, or time required for contraction of wound area to one-half the original.

1.3.5 Ultrastructural, histologic and light scattering studies

Biopsy specimens were obtained one year after surgical procedures from grafted sites, from scars resulting from closure of ungrafted full-thickness wounds, and from site-matched normal skin. Specimens were finely minced, fixed in 4% glutaraldehyde and postfixed in osmium tetroxide, and embedded in an Epon-Araldite mixture. Ulthathin sections were stained with uranyl acetate and lead citrate and examined with a JEOL JSM 10J transmission electron microscope. Small-angle light scattering measurements (SALS) of thin (histological) sections were conducted using a laser beam [24].

1.4 Results

Values of the wound half-life, $t_{1/2} = 8 \pm 1$ days, observed in our present study with ungrafted wound controls, compares well with $t_{1/2}$ values of 7 days which we estimated from independently obtained data with guinea pigs [25]. Ungrafted wounds eventually contracted fully, forming linear scars [6,7]. Wounds covered with full-thickness autografts showed contraction only to about 80% of original area by about Day 30 and subsequently expanded over the next six months to an area slightly larger than the original due to growth of the animal [6].

Control of the mean pore diameter $\overline{d}$ of CG copolymers was a very effective procedure for delaying the onset of wound contraction (Figure 1). A series of cell-free copolymers was prepared with $\overline{d}$ values varying systematically from less than ca. 1 μm to ca. 800 μm by appropriate control of freeze drying conditions. All copolymers in this series were exposed to 0.25% (w/w) glutaraldehyde in 0.05M acetic acid for 24 hours at 23°C. Collagenase degradation assays of copolymers in this series gave values of the degradation rate R which averaged 11 ± 4.7 enzyme units. A maximum increase in $t_{1/2}$ up to 27 ± 2 days occurred when the mean pore diameter ranged between 20 ± 4 μm and 125 ± 35 μm (Figure 1).

The degradation rate of CG copolymers affected the kinetics of contraction independently from the mean pore diameter (Figure 2). A series of cell-free copolymers was prepared with degradation rate values varying from 2.6 ± 0.6 enzyme units to ca. 200 enzyme units by control of the glutaraldehyde crosslinking step. All copolymers in this series were freeze dried under

Table 1: **Effect of Cell Density of CG Copolymers Grafts on Epidermal Confluence**

No. cells/cm^2 graft area	Days to confluence
0	No confluence
$5\times10^4(\pm10\%)$	20.5±11
2×10^5	14.5±3
5×10^5	12.6±2
1×10^6	12.0±2

virtually identical conditions. Pore size determination for these polymers gave $\bar{d}$ values which averaged 450 ± 60 μm. Based on an arbitrary level of $t_{1/2} \geq 15$ days (twice the value for the ungrafted control) we estimated from (Figure 2) an upper cut-off point of 140 ± 25 enzyme units. Above this limiting value, $t_{1/2}$ rapidly decreased, approaching the value for the ungrafted control. The sensitivity limit of the assay was ca. 1 enzyme unit.

Morphogenetic activity was shown by CG copolymers which not only possessed values of the mean pore diameter and enzymatic degradation rate within the critical limits prescribed by Figures 1 and 2 but were also seeded with dermal and basal epidermal cells prior to grafting. When grafted with CG copolymers which had been seeded with at least 5×10^4 cells per cm^2 of graft area, the wounds initially displayed contraction kinetics which were roughly similar to those of cell-free, contraction-inhibiting CG grafts (Figure 3). The onset of contraction occurred on Day 10 ± 1. The contraction rate then reached a maximum and eventually slowed down until the wound perimeter showed almost no change between Days 35 and 50. Thereafter, the wound perimeter expanded at a rate significantly in excess of the normal growth rate of the animal until it asymptotically reached $72 \pm 5\%$ of the original area (Figure 3). Neoepidermal confluence was usually detected at about 2 weeks or less following grafting as formation of a thin, shiny surface comprising layers of *stratum corneum* which could be removed and identified microscopically. Light microscopic studies also showed that formation of a new dermal layer proceeded underneath the neoepidermis over a period of several weeks. After about 200 days the wound perimeter, itself consisting of a thin layer of scar tissue, eventually circumscribed an area of tissue, up to 16 cm^2 with the largest grafts, which grossly appeared identical in color, texture and touch to intact skin outside the wound perimeter with the exception that the new skin was entirely hairless (Figure 4). The gross appearances of the scarred line perimeter and of the tissue area within were similar to corresponding features of the autograft.

The time to reach neoepidermal confluence as well as the kinetics of wound contraction were strongly affected by the density of cells inoculated in the CG copolymer at the time of grafting. Table 1 shows that an increase from 5×10^5 to 1×10^6 cells/cm^2 did not significantly change the time for neoepidermal confluence from the shortest value recorded in our study, 12 ± 2 days ($n = 5$). However, decrease in the cell density down to 5×10^4/cm^2 led to the significantly increased time for neoepidermal confluence of 20.5 ± 11 days. Wounds grafted with unseeded, contraction-inhibiting copolymers did not show epidermal confluence and, following a delay in onset of contraction, eventually closed completely (Figure 3).

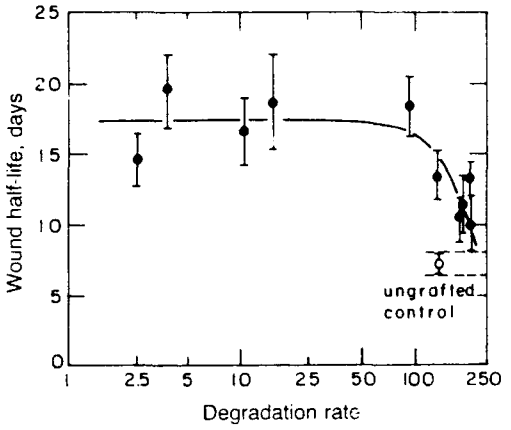

Figure 1: Variation of the skin wound half-life with degradation rate R of CG copolymer used as the graft. The degradation rate is in empirical units, which are defined in the text.

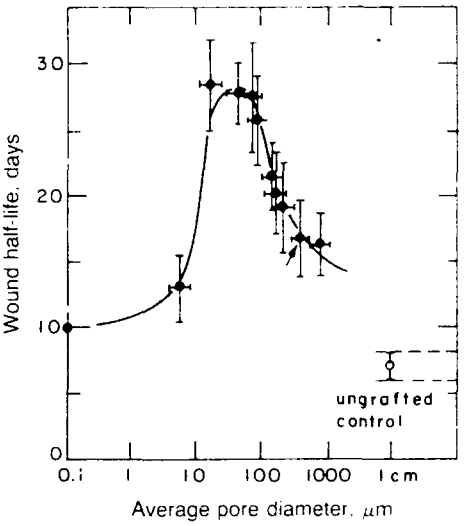

Figure 2: Variation of the skin wound half-life (the time required for a wound to contract to 50% of the original area) with the average pore diameter of CG copolymer used as the graft. The arrow marks the average pore diameter of the copolymer series used to obtain the data in Figure 1.

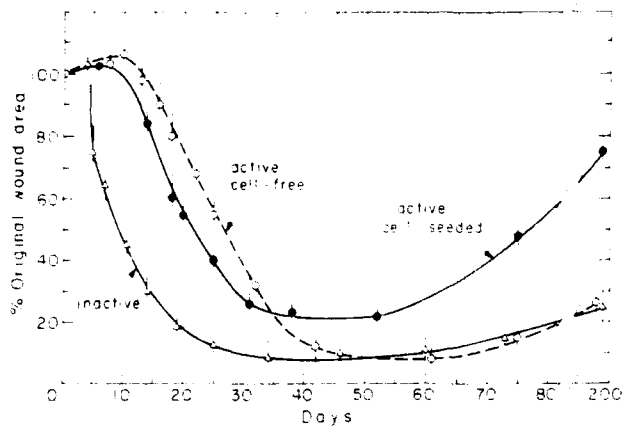

Figure 3: Change in the original wound area with time observed which full-thickness guinea pig skin wounds were grafted with inactive CG copolymers (△), active cell-free CG copolymers (○), and active cell-seeded CG copolymers(●).

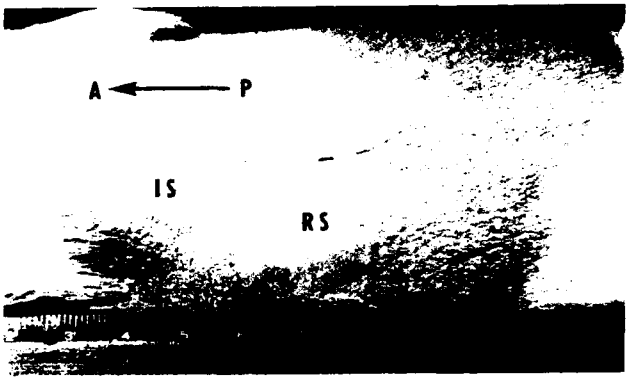

Figure 4: Regenerated guinea pig skin (RS), obtained by grafting a 2 cm × 3 cm full-thickness wound with an active cell-seeded CG copolymer, occupies an area of *ca.* 6.5 cm^2 and has no hair follicles, whereas intact skin (IS) does. The anterior-posterior (AP axis of the live animal (155 days after grafting) is shown. The scale is marked in cm.

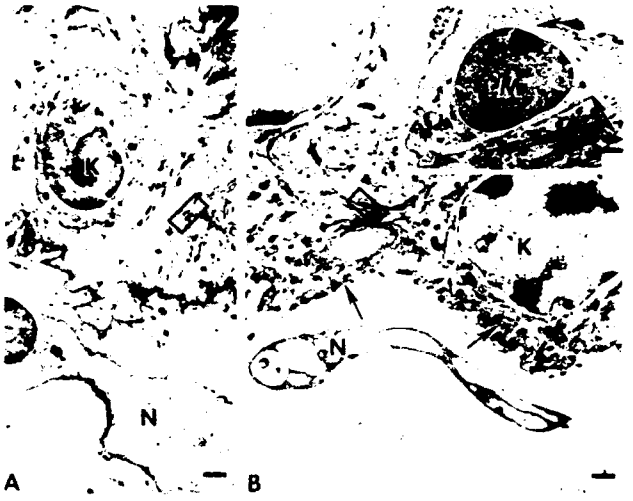

Figure 5 **A**: Normal guinea pig skin. The epidermis is formed by keratino cytes (K) joined by junctional complexes (desmosomes — enclosed by rectangle). Note the characteristic unmyelinated nerve fiber (N) within the superficial dermis. (×3250). **B**: Regenerated skin 14 months after grafting. The neoepidermis is formed by keratinocytes (K) that are identical to intact control skin in **A**. Desmosomes (enclosed and basal lamina (arrows are well-formed and normal in appearance. Melanocytes (M in *Inset*) containing characteristic melanosomes (arrows in *Inset*) also repopulate the neoepidermis, where they normally function in pigment production and donation. A dermal nerve fiber (N), similar to those of normal skin, is also observed (×5400; *Inset*, ×3250). (Bar = 1 μm.)

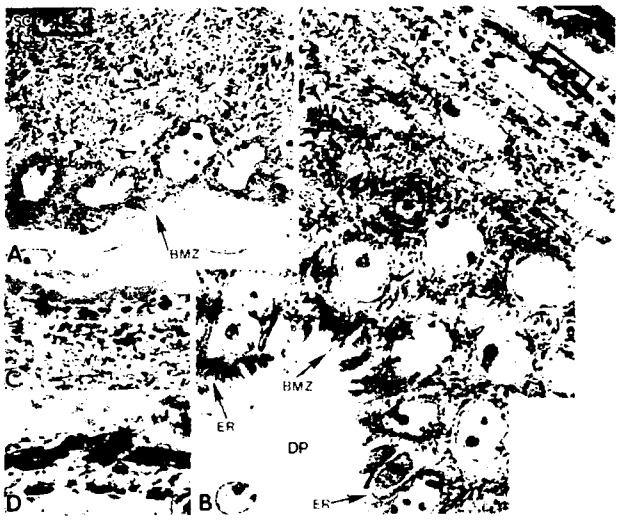

Figure 6: Comparison of the ultrastructure of full-thickness normal guinea pig epidermis **A** and regenerated epidermis 1 year after grafting **B** (identical magnifications). The photographic montage in **B** demonstrates an epidermis that is thicker and contains many more nucleated cell layers than in normal skin **A**. In addition, in contrast to normal epidermis **A** and **C**, keratohyaline granules (enclosed by rectangle) beneath the stratum corneum (SC) of reconstituted epidermis are large and show irregular contours in **D**. DP dermal papilla; BMZ, basement membrane zone; ER, epidermla rete ridges, (**A** and **B**, ×1200; **C** and **D**, ×2500.)

Figure 7 *(right)*: Comparison of collagen fiber and fibroblast orientation in scar **A** and regenerated dermis **B** after 1 year. In scar, fibroblasts (F), collagen bundles (C), and thinned and fragmented elastic fibers (arrowhead) are aligned in parallel with the horizontal axis of the overlying epidermal layer (EPI, double arrow). In regenerate dermis, fibroblasts and collagen bundles are randomly aligned with respect to the epidermal axis, a configuration also observed in normal dermis. In addition, elastic fibers (arrowheads in **B**) are delicate and nonfragmented, suggesting relatively recent synthesis. (×3500.)

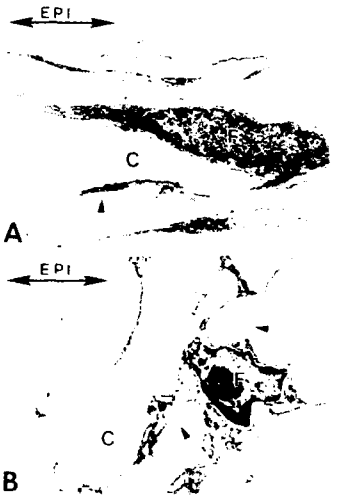

A brief, comparative morphological study of one-year-old guinea pig skin, scar and newly synthesized skin by electron microscopy appears in Figures 5-7. Partly regenerated skin (Figure 5B) was remarkably similar to normal guinea pig skin (Figure 5A) in most respects. The epidermis of regenerated skin was variably hyperplastic and all cell layers were normal in maturation sequence and relative proportion (Figure 6B). Keratohyaline granules of the neoepidermis were generally larger and more irregular in contour than those of the normal granular cell layer (Figures 6C and 6D). Langerhans cells and melanocytes (Figure 5B), normal constituents of the epidermis, were observed in new skin, as were also a well-formed rete ridge pattern and interdigitations with dermal papillae (Figure 6B). In contrast, scar showed marked thinning or atrophy of the epidermis as well as loss of rete ridges and associated dermal papillae. The dermis of regenerated skin exhibited elastic fibers but, unlike the thinned and fragmented fibers seen in scar (Figure 7A), they exhibited a delicate particulate structure (Figure 7B). The collagen fibers forming the dermis in scar were highly oriented in the plane of the epidermis and were interspersed with elongated fibroblasts (Figure 7A), whereas in regenerated skin the fibroblasts were not elongated nor were the collagen fibers highly oriented in the plane of the epidermis. Small unmyelinated nerve fibers were present within dermal papillae in close approximation to the epidermis in both normal and regenerated skin (Figures 5A, 5B); these were not prominent features of scar tissue. However, neither regenerated skin nor scar had hair follicles or other skin appendages. SALS measurements quantitatively confirmed the presence of very low orientation of collagen fibers in normal dermis, moderate orientation in regenerated dermis and very high orientation in scar [24].

1.5 Discussion

The ability of CG copolymers to inhibit the onset of wound contraction depends on their persistence as insoluble networks over a critical period. The observation that wound contraction is delayed if the degradation rate of the copolymer is lower than a critical limit (Figure 1) is most simply interpreted by postulating that the activity of the macromolecular network partly depends on its resistance to rapid solubilization. Alternatively, the data show that CG copolymers do not delay contraction if grafted in a rapidly degradable form. The requirement of a minimum average pore diameter for observation of contraction-inhibiting activity (Figure 2) can be explained most simply in terms of adequately large pore channels for migration of seeded cells. The observed requirement for a maximum average pore diameter, above which the contraction-inhibiting activity of CG copolymers nearly vanishes, probably reflects a requirement for maintenance of a minimal specific surface (cm^2/g) for the insoluble matrix. The specific surface of the copolymers decreases greatly with increase in average pore diameter. The probable importance of specific surface suggests that a critical density of binding sites on the surface of pore channels of CG copolymers is required in order for a sufficient number of cell-copolymer interactions to occur. The combined data (Figures 1 and 2) identify a singular developmentally active factor, an insoluble chemical analog of ECM with well-defined physicochemical structure.

Inhibition of onset of wound contraction can be most simply interpreted in terms of a specific interaction between the model ECM and the myofibroblast [28] or a precursor cell. Wound contraction probably takes place by transfer of mechanical forces over the scale of the wound. Such transfer occurs if the myofibroblast population is modelled as an uninterrupted three-dimensional network, bonded either by direct intercellular junctions or by cell-ECM-cell bonds, which extends over the entire perimeter of the wound or by an uninterrupted network

of matrix components extending around the wound perimeter [26]. Ongoing studies suggest strongly that the transfer of force along the perimeter is of greater consequence than transfer of force acorss the wound bed of a contracting wound [27] The specific interactions between CG copolymers and the cell population of the wound bed are under study. Results of another ongoing study, to be reported elsewhere, suggest strongly that the regenerated epidermis derives from the seeded cells rather than from epithelial cells migrating from the wound edge.

Regeneration of the dermis does not occur spontaneously in the adult mammal [6,7]. The epidermis regenerates spontaneously provided there is a dermal substrate, over which it can migrate [6,7]. Our study shows that a new dermis and a new epidermis can be simultaneously regenerated in a fully excised skin wound provided that the muscle wound bed has been grafted with a highly specific model ECM inoculated with autologous skin cells. Although the regenerated skin is only partly a replica of normal skin, it is significantly different from scar and therefore its synthesis constitutes an unusual morphogenetic event. Clearly, the observed morphogenesis is partly under the control of the model ECM identified in this study. Acting as if it were a transient basal lamina, this model ECM probably mediates the specific interaction between epithelial and mesenchymal cells seeded into it and thereby induces normal tissue differentiation and development in an adult mammalian model where such processes do not spontaneously occur [30].

One of the unseeded CG copolymers which induced morphogenesis of skin in this study has been successfully used as a graft to treat major burns in humans in a multicenter randomized clinical trial[10,31,32]. Furthermore, a series of unseeded CG copolymers with systematically varying structures have induced functional regeneration of the rat sciatic nerve when they were used to bridge large gaps (10 mm and 15 mm) in the transected nerve [33]. The available evidence suggests strongly, therefore, that these copolymers, acting as a temporarily insoluble growth factor, may directly control crucial differentiation steps in a variety of developmental processes.

2 Cell Interactions with a CG Copolymer Matrix Which Induces Dermal and Epidermal Regeneration in Full-Thickness Skin Wounds. Exploratory Ultrastructural Study.

G.F. Murphy, D.P. Orgill and I.V. Yannas

2.1 Abstract

We have sequentially documented the early morphologic events that result in partial regeneration of the adult guinea pig dermis. This phenomenon occurs when a full-thickness skin wound is grafted with a highly specific collagen-glycosaminoglycan (CG) copolymer which has been seeded with autologous dermal and epidermal cells. By day 7, ultrastructural analysis disclosed highly organized associations between mononuclear cells and CG fibers involving prominent extension of pseudopod-like processes toward the fiber surface. Spatial organization of cells was not evident in ungrafted wounds. By day 10, more than 50% of the CG grafts had been degraded and extensive neovascularization was observed in various stages of formation. By day 14, dermal fibroblasts in the graft site demonstrated random alignment of long axes, and a minor fraction ($< 10\%$) exhibited features of myofibroblasts. A majority ($> 50\%$) of dermal fibroblasts in ungrafted wounds were identified as myofibroblasts at this time, and their axes were regularly aligned in parallel with the overlying epidermal layer. Scattered CG copolymer fragments were engulfed by macrophages by day 14, and complete dissolution occurred by day 21. Dermal blood vessels formed a discrete, subepidermal plexus oriented parallel to the epidermal plane by days 14 to 17 in grafted wound beds but not in ungrafted ones. Progressive, randomly oriented collagen deposition occurred at graft sites during the 1st year, whereas collagen fibers in ungrafted wounds were aligned in a horizontal plane atypical of a forming scar. By 1 year, the graft sites resembled normal dermis, with well-defined dermal papillae, normal anastomosing superficial vasculature, nerve fibers, and random collagen fiber morphology. Wound sites at this juncture resembled a mature scar, with a flattened dermal-epidermal interface; rare and disorganized vessels and nerves; and collagen fibers parallel to the epidermis. This investigation demonstrates the critical importance of highly specific extracellular matrix in induction of dermal morphogenesis.

2.2 Introduction

This pilot study was an ultrastructural survey of cell-CG copolymer interactions during the three-week period following grafting of a full-thickness skin wound in the guinea pig. A specific objective was to explore the three-dimensional character of the cell-copolymer interaction and to compare it with the spatial organization of cells in granulation tissue (ungrafted control).

2.3 Methods

The standard guinea pig full-thickness skin wound was prepared as previously described and was either grafted with a CG copolymer or covered with a Xeroform gauze (control). The average pore diameter, the degradation rate in collagenase and the density of cells seeded into the copolymer were all within the restrictions that were described in a previous study. One year after grafting, the resulting new epidermis and dermis resembled physiological skin rather than scar. However, hair follicles and other skin adenexa were missing from regenerated

skin. Ultrathin sections stained with uranyl acetate and lead were viewed with a Hitachi HU12 transmission electron microscope. A minimum of 100 random fields were examined and photographed at low magnification (1200X) for each time point. Light microscopy was also performed and was based on one-micron sections stained with Giemsa. Sampling of tissue for ultrastructural analysis focused on dermal elements, and epidermal events were not documented comprehensively in the present study.

2.4 Results

By Day 7 we observed highly organized associations between mononuclear cells and CG fibers involving prominent extension of filopodia toward the fiber surface. Spatial organization of cells was not evident in ungrafted wounds. By Day 10 more than 50% of the graft had been degraded and extensive neovascularization was observed in various stages of formation. By Day 14 dermal fibroblasts in the graft site demonstrated random alignment of long axes, and a minor fraction ($< 10\%$) exhibited features of myofibroblasts. A majority ($> 50\%$) of dermal fibroblasts in ungrafted wounds were identified as myofibroblasts at this time, and their axes were regularly aligned in parallel with the overlying epidermal layer. Scattered CG copolymer fragments were engulfed by macrophages by Day 14, and graft fragments were not visible by Day 21. Dermal blood vessels formed a discrete, subepidermal plexus oriented parallel to the epidermal plane by Days 14 to 17 in grafted wound beds but not in ungrafted ones. Progressive, randomly oriented collagen deposition occurred at graft sites during the first year, whereas collagen fibers in ungrafted wounds were aligned in a horizontal plane typical of a forming scar. By one year the graft sites resembled normal dermis, with well-defined papillae, normal anastomosing superficial vasculature, nerve fibers, and random collagen fiber morphology. After one year ungrafted sites resembled mature scar, with a flattened dermal-epidermal interface, rare and disorganized vessels, and collagen fibers oriented parallel to the epidermis.

2.5 Discussion

This pilot investigation has highlighted the apparently very intimate and clearly three-dimensional interactions between cells in the grafted woundbed and the CG copolymer. These three-dimensional scaffolding structures clearly merit further study. Our findings suggest that the observed randomness in orientation of cellular axes in the presence of the graft is dictated by the precise features of the pore structure of the copolymer since, in the absence of the latter, cells (myofibroblasts) align themselves in the plane of the epiderrmis. We speculate that these randomly aligned cellular axes persist after the copolymer has degraded and their orientation is possibly reflected in the orientation of collagen fibers which are eventually deposited to form the mature, regenerated dermis. According to this model, collagen fiber synthesis coincides spatially with the myofibroblast network. This model suggests the possibility that collagen is synthesized only by the cells which make effective contact with the undegraded copolymer and which, therefore, have a shape similar to that of the copolymer fiber to which they are attached via extensive filopodia contact. Since, according to this model, collagen is synthesized only near the surface of the copolymer fibers, it is suggested that the random orientation of the copolymer fibers becomes "imprinted" on the orientation pattern of newly synthesized dermal collagen fibers.

3 Disruption of Contractile Cell Network in Healing Skin Wounds by CG Copolymers

K. Troxel, I.V. Yannas and coworkers

3.1 Ongoing Study. Summary

An immunoperoxidase staining study was conducted in order to evaluate the possible mechanism of the delay in onset of woundbed contraction by CG copolymer grafts. Contractile cells known as myofibroblasts were immunohistochemically stained using a monoclonal mouse anti-alpha smooth muscle actin IgG for the primary antibody (Sigma SIH903). The goal of the study was to determine the time of appearance and relative numbers of myofibroblasts in the CG grafted wounds as compared to control wounds prior to the onset of contraction of the woundbeds. Tissue samples were taken from grafted and ungrafted wounds prior to and during contraction of the wounds.

Estimates of the numbers of total cells and myofibroblasts per wound cross-section were made by counting the nuclei on a series of photographs. Nuclei with red-stained cytoplasm were counted as myofibroblasts. Nuclei without stained cytoplasms were also counted in order to calculate the total number of cells. The average number of nuclei per photograph was divided by the area per photograph and multiplied by the cross-section area of the grafted or ungrafted wound tissue to find the total number of cells or total myofibroblasts per wound cross-section.

The immunohistochemical stain revealed that the myofibroblasts first appear in CG grafted wounds and in control wounds around the same time, around day 4-5. Comparisons of the number of cells per cross-section of CG grafted versus control wounds show that the number of cells that are invading the wounds are similar before day 6, after which there is a dramatic rise in the number of cells in the CG grafted wound. There was also a rise in the number of myofibroblasts after day 6 in grafted wounds compared to ungrafted wounds (Figures 8A and 8B).

These data show that the CG graft does not impede the movement of cells into the woundbed, nor does it delay the differentiation of cells to the myofibroblast phenotype. This finding contradicts the suggestion [29] that CG grafts induce depletion of myofibroblasts from the population of cells in the woundbed. The delay of the onset of contraction by the CG graft is most likely caused by a disorientation of the long axes of the contractile cells, as the latter become intimately associated with the randomly oriented surfaces of pore channels in the CG matrix (Figures 8A and 8B).

These studies suggest that the CG grafts significantly change the wound healing response by dramatically disorienting the long axes of the contractile cells in the woundbed. These cells become very intimately associated with the surface of fibers in the CG graft.

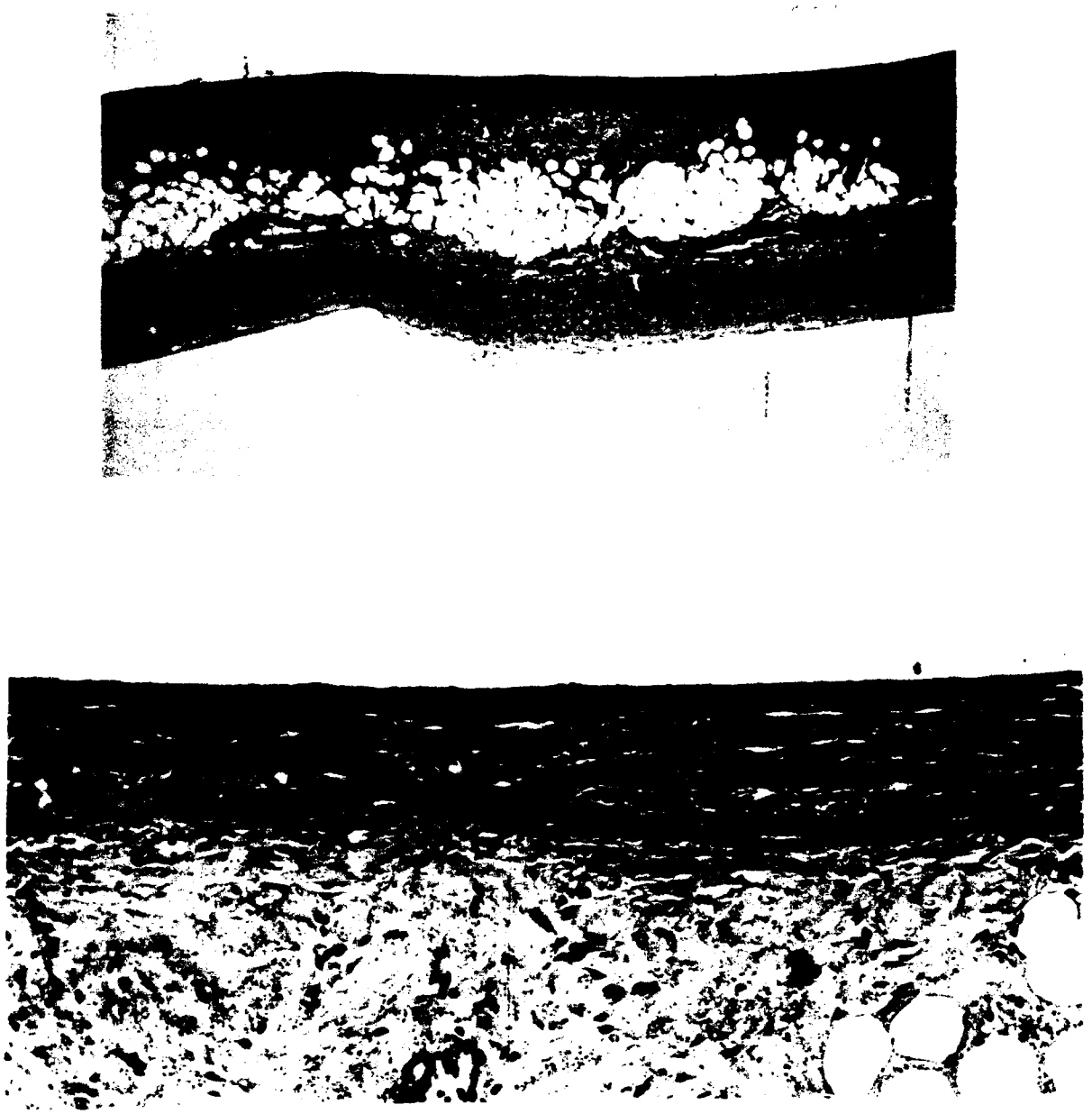

Figure 8A: Granulation tissue (ungrafted wound bed) undergoing vigorous contraction, day 10. Tissue was immunoperoxidase stained (brown stain) with anti-α smooth muscle actin using AEC as substrate and counterstained with Gill's 3X Hematoxylin. Top: $\times 36$. Bottom: $\times 180$.

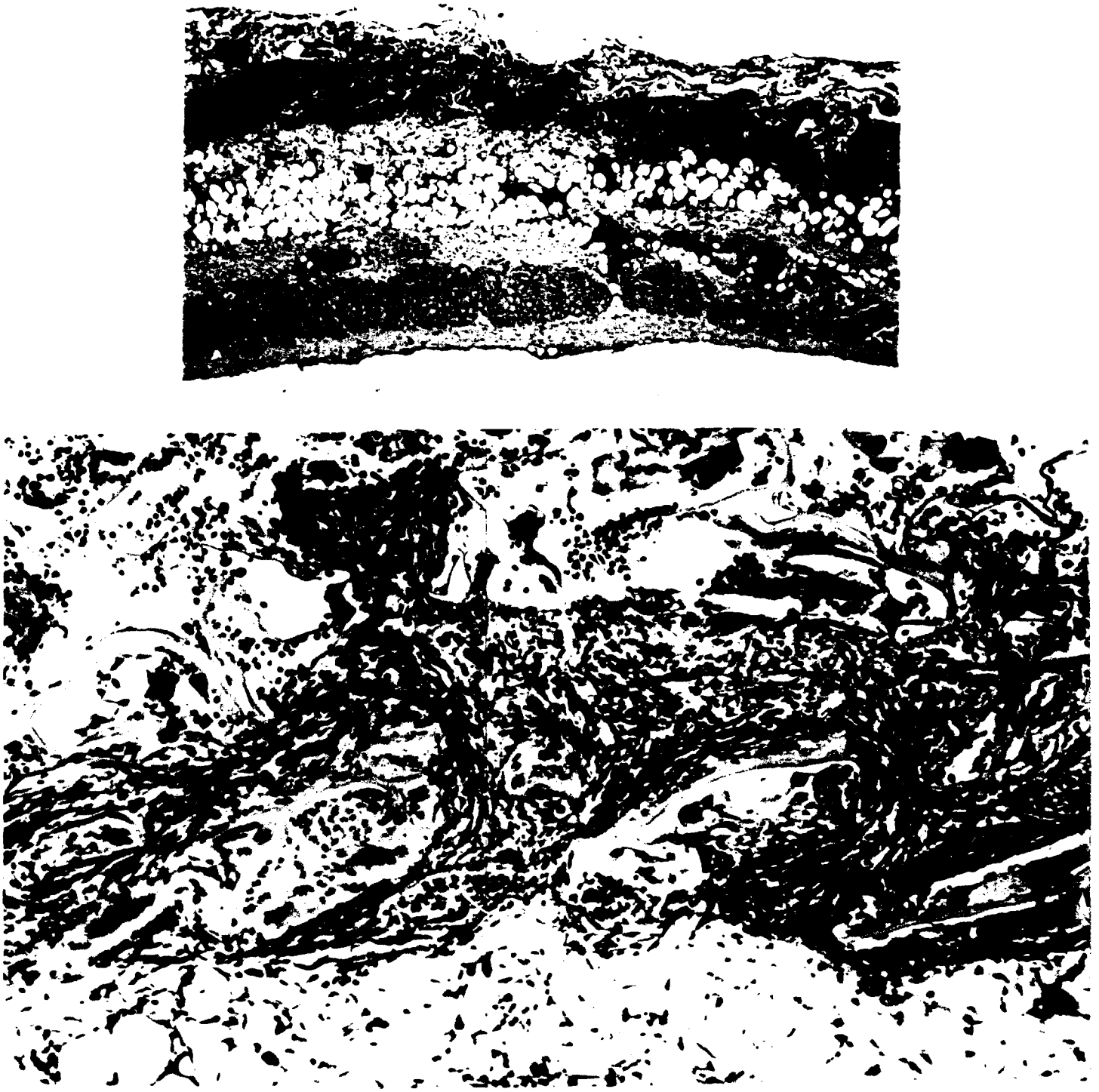

Figure 8B: Wound bed grafted with a CG copolymer on day 9. Contraction has not been initiated. The tissue was immunoperoxidase stained (brown stain) with anti-α smooth muscle actin using AEC as substrate and counterstained with Gill's 3X Hematoxylin. Top: ×36. Bottom: ×180.

4 Scattering of Light from Histological Sections: A New Method for the Analysis of Connective Tissue

A.G. Ferdman and I.V. Yannas

4.1 Abstract

We have developed a light scattering technique which can be used to analyze the degree of orientation and diameter of collagen fibers in histological sections of connective tissue. Scattering patterns obtained by transmitting laser light through sections of tissue contain information both on the orientation and size of the constituent collagen fibers. Analysis of the azimuthal intensity distribution of scattered light yields numerical values of the orientation index, S, which is chosen to vary between 0 for randomly oriented fibers and 1 for a perfectly aligned arrangement. The average diameter of the collagen fibers is calculated from the scattering angle at which the intensity reaches its first minimum. These measurements are independent of the nature of histological stain which may have been used to color the tissue section. The procedure is illustrated by measurements obtained with sections of the guinea pig dermis and of control scar. Light scattering can complement the analysis of tissue architecture performed with the light microscope.

4.2 Introduction

The diameter of collagen fiber bundles in connective tissue is equal to roughly between ten and fifty times the wavelength of visible light [35]. For this reason, collagen fiber bundles scatter light at small angles, roughly between 1° and 6° [36]. Light scattered from histological sections of dermis produces a scattering pattern which contains information on the orientation and size of the constituent fibers. These patterns, which can be viewed directly by transmission, are simple to interpret and can be used to evaluate readily the average morphological features of the tissue. We have developed a light scattering method capable of analyzing connective tissue and have used it to study dermal [24] and other tissues.

The procedure is illustrated most simply by use of a conventional histological section (approximately 4 μm in thickness) of scarred guinea pig skin adjacent to intact dermis. When the light passes through the dermis the scattering pattern is characteristically elliptical in appearance (see Figure 9). Translation of the beam from the region of dermis to that of scar (in the same tissue section) yields an elongated pattern, indicative of high orientation of fibers in this region. The difference in the two scattering patterns can be used to obtain a numerical measure of the difference in orientation between the two tissues.

The degree of orientation is defined by an orientation index, S, which has an upper limit indicative of perfect orientation along a given axis and a lower limit corresponding to an ideally random orientation. A particularly useful definition for S is:

$$S = 2(\cos^2 \alpha) - 1 \tag{1}$$

where α is the angle between an individual fiber and the mean axis of the fibers, and $(\cos^2 \alpha)$ denotes the square cosine of α averaged over all the fibers in the sample. The coordinate system for light scattering from a tissue section is shown in Figure 10. Since $(\cos^2 \alpha)$ equals 1/2 for a random arrangement of fibers and 1 for a perfectly aligned arrangement, S will vary

from 0 to 1, respectively. The final expression for S used to calculate the orientation index from experimental data is:

$$S = 2\frac{\int_0^{\pi/2} \mathrm{I}(\beta)\cos^2\beta \mathrm{d}\beta}{\int_0^{\pi/2} \mathrm{I}(\beta)\mathrm{d}\beta} - 1 \qquad (2)$$

where the angle β (defined in Figure 10) is the rotation angle at which the intensity of scattered light, I, is measured.

Fiber diameter d was calculated by approximating the scattering due to collagen fibers as diffraction from a randomly spaced collection of slits with a nonrandom orientation distribution:

$$d = \frac{l}{\sin\theta_1} \qquad (3)$$

where l is the wavelength of light and θ_1 is the scattering angle at which the intensity reaches its first minimum.

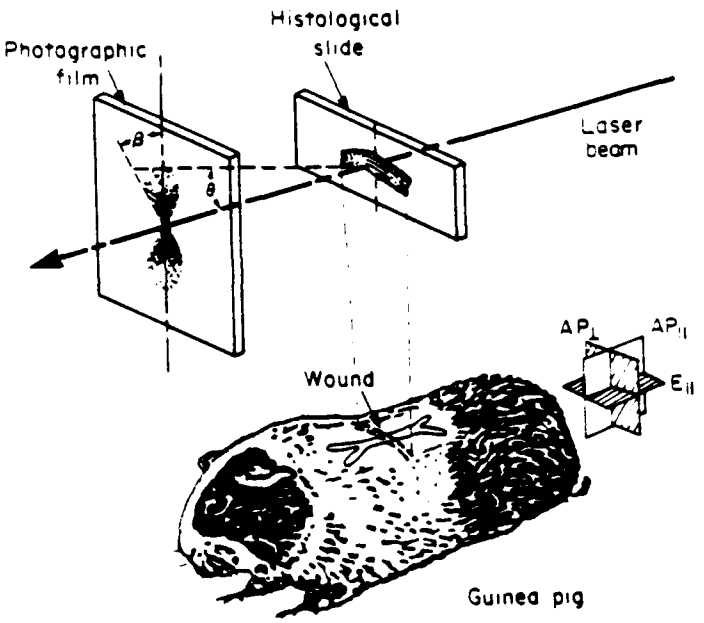

Figure 9 *(right)*: A laser can extract information from a histological slide. When a laser beam is passed through a histological section of tissue, the constituent fibers act as slits diffracting light in directions perpendicular to the orientation of the fibers. By passing a laser beam through a section of tissue, the scattering pattern can immediately be used to determine the preferred alignment direction of the fibers, to measure the degree of alignment of the fibers, and to measure the diameter of the fibers. As the laser beam (depicted by circles) was passed through the section shown here, the corresponding patterns were obtained. The patterns reflect the orientation and size of the fibers in the tissue.

4.3 Materials and Methods

He-Ne laser light was passed through a spatial filter and then scattered by the sample. The spatial filter was constructed using two convex lenses of focal lengths f_1 and f_2 and a 100 μm pinhole. The filter was used to produce a beam with a Gaussian profile and diameter d given by $d_i f_2/f_1$, where d_i is the initial beam diameter and f_1 and f_2 are the focal lengths of the first and second lenses, respectively. Beam diameter d was defined to include 95% of the beam's intensity. With appropriate positioning of the lenses the beam could be set to diameters between 50 μm and 1.5 mm. Useful beam diameters, however, ranged between 100 μm and 1 mm. Histological samples were mounted on a stage allowing translation in directions perpendicular to the beam axis. Scattering patterns were recorded directly onto instant film (Polaroid Type 52, Cambridge, MA) (Figure 11).

The intensity of the scattered light was measured with a silicon photodiode (0.81mm^2 active area, catalog #SGD-040B, EG&G, Billerica, MA) mounted on a stage capable of recording either scattering angle θ or rotation angle β. A plate with a 3mm diameter hole was placed

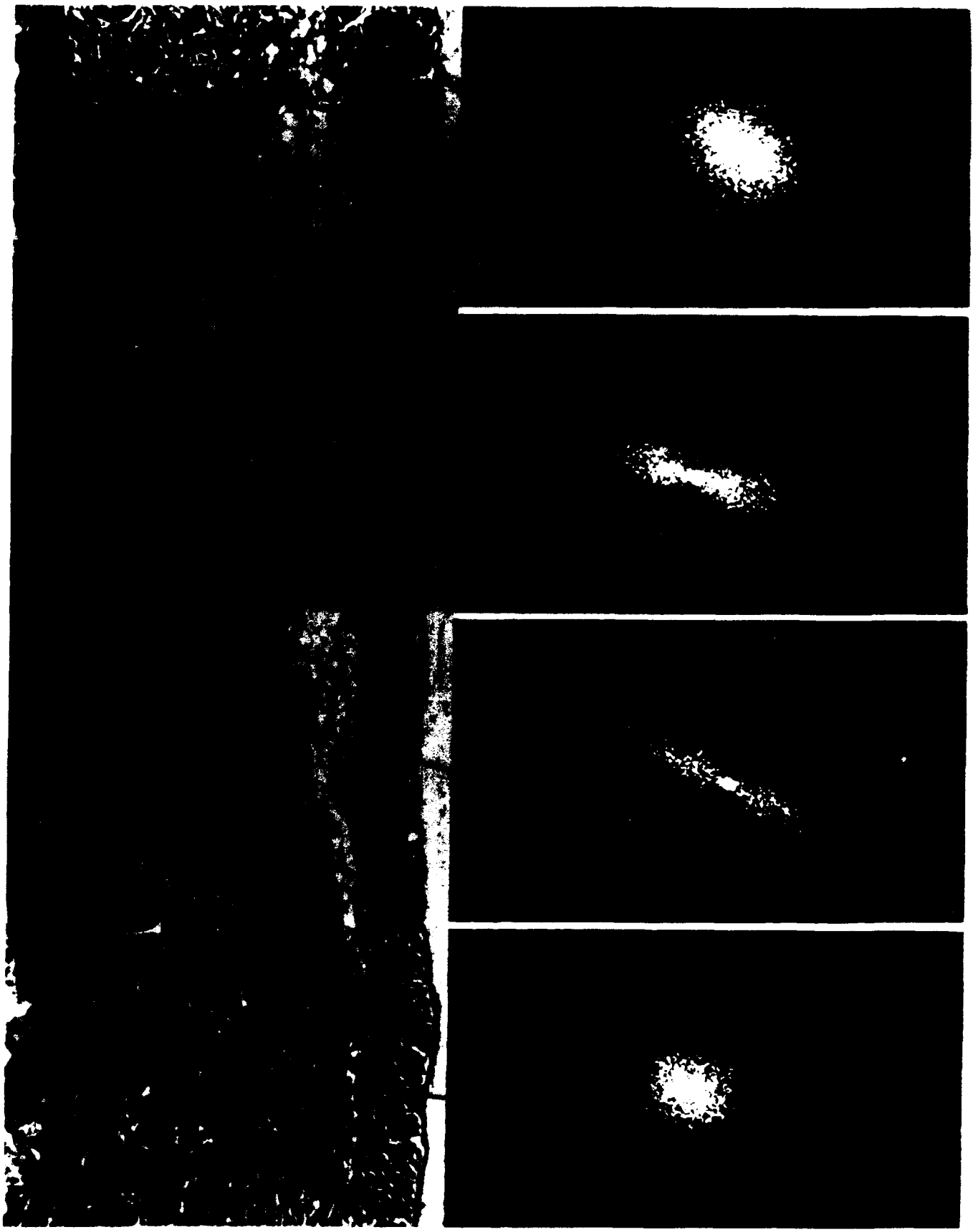

Figure 10

Figure 10 (*preceeding page*): Light scattering from a histological section. The laser beam passes through a histological section which is represented here as a slice of tissue perpendicular to the long axis of the healing wound. The resulting pattern is viewed on the photographic plane and has associated with is the characteristic scattering angle θ and the azimuthal (or rotation) angle β. See also Figure 9. The intensity can be measured along either one of these angles, such as by fixing θ and varying β to obtain $I(\beta)$, or by fixing β and varying θ to obtain $I(\theta)$. $I(\beta)$ contains information on the orientation of constituent fibers whereas $I(\theta)$ contains information on their size. Animal planes $AP_{\perp}$, $AP_{\parallel}$, and $E_{\parallel}$ are shown here to correspond to sections cut perpendicular to the anterior-posterior axis, along the axis, and parallel to the epidermal plane, respectively.

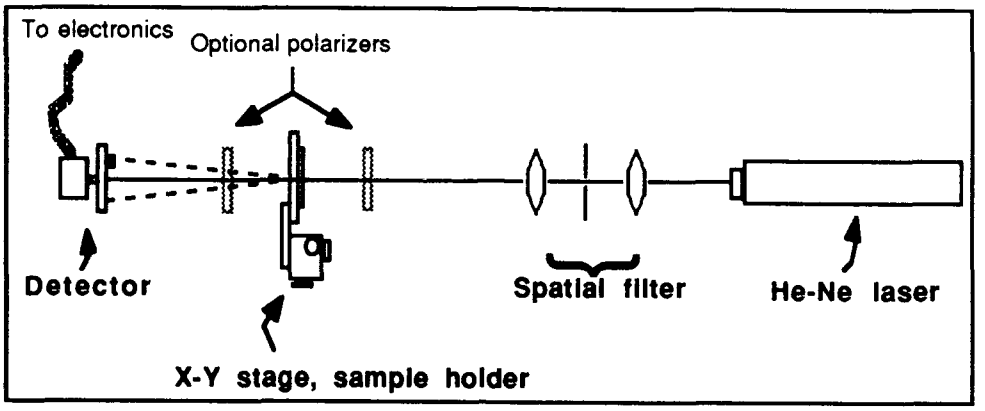

Figure 11 (*above*): Schematic of the optical bench used to measure the angular distribution of light scattered from tissue sections.

in front of the sample in order to reduce the number of multiple reflection spots reaching the diode. The input voltage noise level of the detector was roughly $0.3\mu V$; typical signal-to-noise ratios were 10^3 or higher. A three-turn standard potentiometer was used to record β; θ was recorded using a linear resistor fixed onto the potentiometer by means of a disk. The photodiode, mounted onto the lever dial of the linear resistor, could either be fixed at a particular rotation angle and moved along the track of the linear resistor or fixed at a particular distance away from the origin and rotated in the plane normal to the light beam. Plots of $I(\beta)$ and $I(\theta)$ were obtained using an X-Y plotter (Plotamatic 715, MFE Corporation, Salem, NH) with the amplified photodiode output plotted on the y-axis and either β or θ recorded on the x-axis.

Samples of normal dermis were obtained from the dorsum of 21 white, female Hartley guinea pigs. Scar tissue was produced in 7 white, female Hartley guinea pigs by excising from the dorsum a 1.5×3.0 cm^2 area down to but not including the *panniculus carnosus*, treating the wounds with Xeroform gauze, and waiting from 6 months to one year for completion of wound healing.

Tissue specimens were stored in 10% buffered formalin for a minimum of 24 hours, bathed in increasing concentrations of alcohol, embedded in paraffin, sectioned, and then stained using standard histopathological technique. Thickness of the sections was approximately 4 μm. Specimens were stained with one of a number of histological stains, although it was found to have little if no effect on the results. Examples of stains used are: Mayer's alum hematoxylin counterstained with eosin, Masson's Trichrome, P.A.S., Voerhoff's. Structurally

Table 2: **Orientation Index and Fiber Diameter of Normal Dermis and Scar**

Tissue	Orientation Index, S	Fiber Diameter, d	
		Light Scattering	Microscopy
Normal Dermis	0.20 ± 0.11	20 ± 7 μm	$26 \pm$ μm
Scar	0.75 ± 0.10	13 ± 5 μm	11 ± 8 μm

similar specimens were obtained by serial sectioning.

4.4 Results

Characteristic scattering patterns obtained from sections of normal dermis and scar which were cut with the plane of the section perpendicular to the anterior-posterior axis are shown in Figure 12. Typical I(β) curves are shown in Figures 13 and 14. The shape of the scattering patterns suggests that scar tissue is highly oriented relative to normal dermis. A significant difference ($p < 0.0001$) in the orientation index between the two types of tissues is reflected in values of S, presented in Table 2.

Values for the fiber diameter of normal dermis and scar obtained by light scattering and light microscopy are compared in Table 2. The diameter of the collagen fibers, as estimated using eqn. (3), were found to correlate well with values obtained by light microscopy.

The results indicate that the fibers in guinea pig scar tissue (healed for periods ranging between 1/2 to one year) are highly oriented and are 40–65% thinner in diameter than normal dermis fibers. Neodermis (synthesized by grafting with a cell-seeded analog of ECM, as described in Section 1 above) had an orientation index between normal dermis and scar (approximately 0.45 ± 0.11) and consisted of fibers 60–75% the diameter of normal dermis.

4.5 Conclusions

By scattering laser light from histological sections of tissue we have been able to obtain information on the degree of orientation and diameter of the constituent collagen fibers. The method successfully measures both the direction of the mean fiber axis in a histological section as well as the degree of orientation of the fibers about the fiber axis. When the method was applied to the study of dermal tissues, it was observed that scar tissue is highly oriented, normal dermis only slightly oriented, and regenerated dermis to have an orientation index between scar and normal dermis. This method facilitated the comparison of various dermal tissues and may therefore serve to optimize the performance of membranes (based on ECM analogs) currently being studied as templates for skin regeneration.

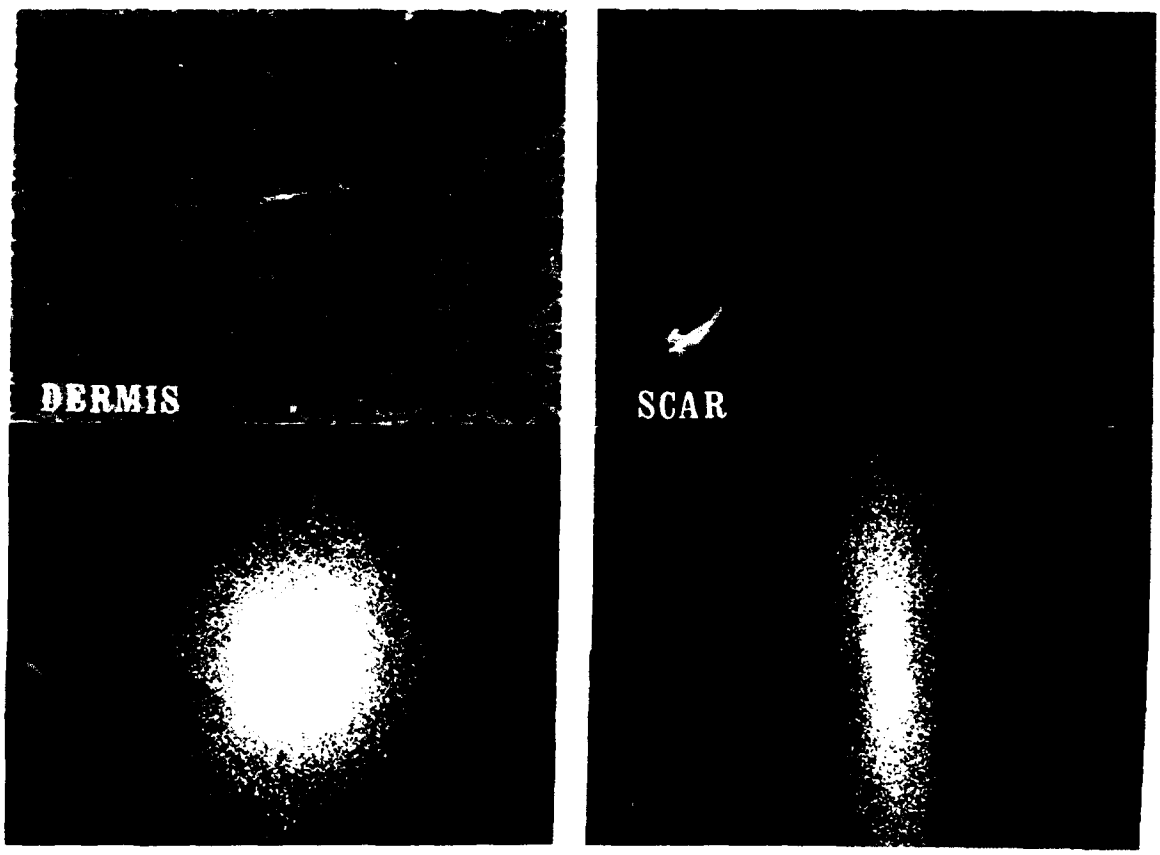

Figure 12: Normal dermis versus scar. The scattering patterns for normal dermis *(bottom left)* and scar (*(bottom right)* reflect the inherent alignment of fibers in the tissue. In the reticular dermis *(top left)*, shown here with cross-sections of two hair follicles, the fiber bundles are thicker and more randomly oriented than in scar *(top right)*: fiber bundle cross-sections evident in the normal dermis tissue section are from fibers pointing in directions other than in the plane of the tissue sections. In scar, the fibers are aligned across the wound and are therefore, in the AP$\perp$ cut (see Figure 10), aligned within the plane of the tissue section. Plots of I(β) obtained from these tissues, shown in Figures 13 and 14, can be used to calculate the degree of alignment of the fibers.

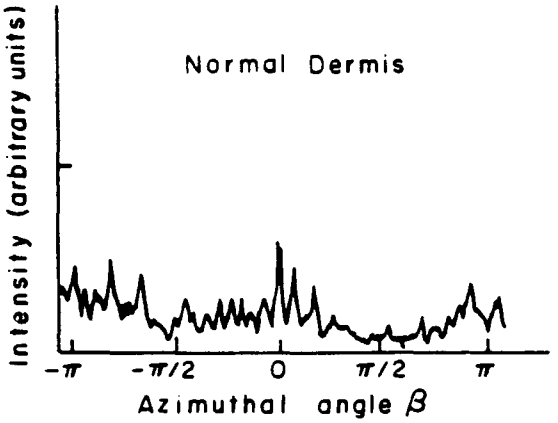

Figure 13: Typical scattering curve for normal dermis. In a typical plot of intensity versus azimuthal angle β for normal guinea pig dermis, the intensity is not a strong function of β; this indicates a nearly random arrangement of fibers in the tissue section. The intensity peaks slightly at 0 and π suggesting that there is a slight alignment of the fibers perpendicular to these angles. Since 0 and π are measured above and below the tissue section, the slight alignment is in a direction perpendicular to the epidermal plane. The plot shown here corresponds to the scattering pattern for normal dermis shown in Figure 12, bottom left.

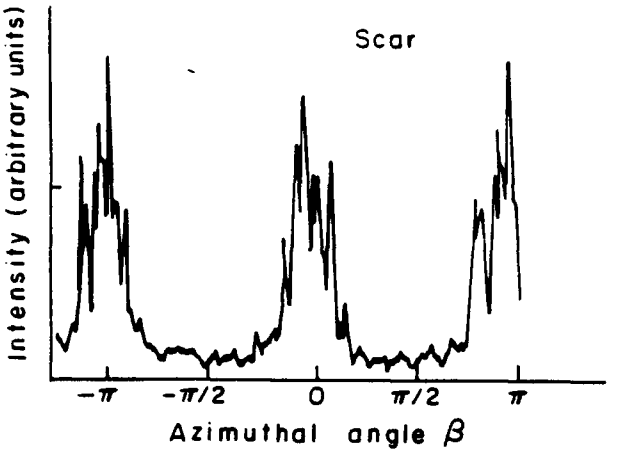

Figure 14: Typical scattering curve for dermal scar. As opposed to the graph shown in Figure 12, the intensity is a strong function of β when obtained from a typical scar. The strong peaks, which occur at 0 and π, indicate a strong preferential alignment of the fibers in a direction perpendicular to these angles. Since 0 and π are measured above and below the tissue section, the strong alignment is in a direction perpendicular to the epidermal plane. The plot shown here corresponds to the scattering pattern for scar shown in Figure 12, bottom right.

5 Attempted Langerhans Cell Depletion of Populations of Epidermal Cells

D. Gebala and S. Izatt

5.1 Abstract

A method for separating the Langerhans cell population from a mixed dermal and epidermal cell population was studied in a preliminary manner. The objective of this research was the design of skin grafts which are donor-independent. It can be hypothesized that the Langerhans cells in the skin are the most significant contributors to rejection of skin grafts. A technique for removal of Langerhans cells would, according to this hypothesis, provide the basis for fabrication of a cell-seeded, nonimmunogenic graft for the regeneration of dermis and epidermis as described in Section 1 (in which autologous cells were used to seed ECM analogs). Several methods were considered before designing a monolayer panning technique for removal of Langerhans cells from epidermal cell preparations. The panning technique was conceptually designed and tested in a preliminary way on the expectation that a monoclonal antibody with high specific affinity for a surface marker of guinea pig Langerhans cells would become available during the course of this study. Such an antibody would have been analogous to the LC antibody (OKT-6) which is known to recognize the CD1a antigen in humans. However, a search showed that no such antibody specific to guinea pig Langerhans cells was available at the termination of the study.

6 Cryopreservation of Epidermal Cells at −80°C

E.M. Skrabut and J. Wong

6.1 Abstract

Cryopreservation of guinea pig epidermal cells was demonstrated at −80° C after 3 days of freezing. This result extended our previous development of a cryopreservation method for epidermal cells at −196° C. Cryoprotection with dimethylsulfoxide at −80° C yielded higher cell viability (90%) than with glycerol (60%). Cryopreservation at −80°C (dry ice) can be accomplished much more conveniently than at −196°C (liquid nitrogen).

7 Use of an Extracellular Matrix Analog to Assess Immunogenicity of Epidermal Cell Allografts

L.S. Ritterbush and I.V. Yannas

7.1 Abstract

A previously developed extracellular matrix (ECM) analog was used to simultaneously study the location of skin immunogenicity and the practicality of a skin replacement therapy. The ECM analog, consisting of a collagen-glycosaminoglycan (CG) copolymer, was used as a carrier of foreign epidermal cells in transplantation experiments in the guinea pig. The objective was to determine whether such cells are the primary agent responsible for skin allograft rejection and therefore whether or not ECM analogs seeded with foreign cells might be used in a skin replacement therapy.

A model of clinical rejection was developed using inbred strain 2 and strain 13 guinea pigs. The model was tested with skin transplants between strains (rejected) and skin transplants between individual animals of the same strain (accepted). The model was then used to assess transplants of epidermal cells only. These transplants were achieved using the ECM analog as a carrier. Strain 2 animals acted as cell donors for strain 13 recipients and vice versa. Cells were seeded into ECM analogs, and the seeded analogs were grafted onto full-thickness wounds.

A quantitative assay for rejection of these grafts was developed using a monoclonal antibody specific for cells involved in rejection. T cells in biopsies from the grafts were labelled with the antibody, and labelled cells were visualized by immunoperoxidase staining. The response was quantified by counting stained cells in histological sections. Staining and counting were also carried out for the following control grafts: skin placed back on the same animal; skin transplanted between strains 2 and 13; skin transplanted within strain 2 or 13; ECM analog seeded with cells returned to the same animal; ECM analog alone; silicone component of ECM analog; and intact skin. The data were analyzed for statistical significance and the following conclusions were drawn with 95% confidence: ECM analogs seeded with foreign cells provoke a much weaker rejection response than does foreign skin; silicone alone causes a high response; all other controls cause a low response, one which is not significantly different than that seen for ECM analogs seeded with foreign cells.

Rejection was assessed qualitatively by gross observation and histological sections. Fourteen animals were grafted using ECM analogs seeded with foreign cells. Twelve showed no gross evidence of rejection between one and two weeks after grafting. Two animals showed severe graft degradation and infection, indicating a rejection response.

Four long-term grafts (ECM analogs seeded with foreign cells) were assessed histologically for evidence of new tissue synthesis. Biopsies obtained 102 days post-grafting showed variable results. Two grafts had formed linear scars. Two grafts had prevented the formation of a linear scar, and showed histological evidence of both new dermal tissue and scar in the healed wound. Transplanting foreign epidermal cells via a nonimmunogenic ECM analog reduced rejection significantly as measured by T cell response. This suggests that dermal components are the primary targets of rejection. This transplantation method appears to reduce rejection to a level which may be clinically acceptable, based on gross observation. The histologic evidence of partial tissue regeneration reinforces the clinical potential of ECM analogs seeded with foreign cells.

7.2 Introduction

There is great need for an immediately graftable, nonimmunogenic material which supplies the function both of the dermis and the epidermis over an indefinite period. Toward this end we have been working toward extending the function of the dermal ECM analog which has been developed [12,37,13]. This ECM analog has already been shown to be capable of promoting the regeneration of an epidermis as well as a dermis when it is seeded with epidermal cells derived from the graft recipient's own epidermis [34]. If cells donated by other individuals or derived from cultured cell lines could be used without provoking rejection, then the problem of availability of non-immunogenic material could be circumvented, and a maximally useful skin replacement therapy would result. ECM analogs could be seeded with cells from any donor or from a cultured cell line and then frozen in storage until needed.

An unresolved issue is the location of skin immunogenicity. Skin contains two major components. One component, the epidermis, is a thin (approximately 0.1 mm) cellular layer at the surface of the body. The other component, the dermis, is a much thicker (approximately 2 mm), underlying layer of connective tissue. The factors which cause rejection could reside in the epidermis, the dermis, or both. If the epidermis is the major source of antigens, then the use of ECM analogs seeded with foreign epidermal cells would require treating the cells to reduce their immunogenicity. Such a treatment would have to be developed; none exists at the present time (See Section 5 above for a conceptual design of a technique for depletion of Langerhans cells from epidermal cell populations). If the dermis carries most or all of the skin's immunogenicity, then ECM analogs seeded with foreign epidermal cells may offer significant clinical potential.

Separating skin into its two components and grafting each individually would seem to be the logical approach to answer this question. However, this experiment suffers from practical limitations. First, separating skin into its two components is not easily accomplished. Extensions of the epidermis, principally hair follicles, extend deep into the dermis. The two layers can be grossly separated quite easily, but treatments necessary to remove residual epidermal elements could remove cellular elements of the dermis which are important to the rejection phenomenon. In addition, grafting of the individual layers of skin does not offer a clinically sound experiment. Epidermis by itself grafted onto full-thickness wounds has been shown not to take well to the graft site [38]. Dermis alone will adhere well to a wound bed but the result is an open wound. An epidermis or epidermal analog must be applied to achieve a closed wound, and this introduces another variable.

The ECM analog offers a means of probing the skin for the location of its immunogenicity. The analog has already been shown to function as dermal scaffold, promoting the regeneration of a new dermis from the wound bed onto which it is grafted [9]. In addition, the ECM analog has been shown to promote the regeneration of an epidermis from seeded epidermal cells, as noted above. This suggests the use of the ECM analog as a nonimmunogenic carrier of foreign epidermal cells to determine whether they are the main culprit in skin rejection. Such a study could provide new information about the location of skin immunogenicity. This information would likely help in the design of an effective skin replacement therapy. If the ECM analog seeded with foreign cells is not rejected, this will indicate that the dermis is the principal carrier of skin immunogenicity. In this event, the ECM analog seeded with foreign cells will have a demonstrated potential for use in a skin replacement therapy.

A preliminary study has produced inconclusive results. Orgill [40] found variable results when epidermal cells in ECM analogs were transplanted between individual guinea pigs of the

Hartley outbred strain. Small (1.5 cm by 3.0 cm) grafts were rejected about 40% of the time, medium (2.0 by 4.0 cm) grafts were rejected about 50% of the time, and large (3.0 cm by 3.0 cm) grafts were rejected about 80% of the time.

We describe below a systematic attempt to assess the immunogenicity of foreign epidermal cells transplanted via ECM analogs. A genetically-defined model of clinical rejection and a quantitative assay for magnitude of rejection have been developed. These have been used to analyze the rejection response to such grafts.

7.3 Materials and Methods

7.3.1 Preparation and Characterization of Extracellular Matrix (ECM) Analog

See Section 1 above for the detailed preparation procedure.

7.3.2 Animal Model

Grafting was carried out on guinea pigs to obtain results which could be compared to previous skin regeneration work performed in this laboratory [40]. These previous studies were carried out on animals of the Hartley outbred strain. The Hartley is a hardy, short-haired, white (pseudo-albino), widely available strain. The outbred nature of the Hartley strain means that it is not genetically controlled; some individuals are more closely related than others.

Development of a controlled, reproducible clinical rejection model required the use of animals known to consistently differ at genetic loci responsible for transplantation. This suggested the use of inbred animal strains. A search of laboratory animal resources in the U.S. revealed that only two inbred strains of guinea pig, strain 2 and strain 13, are maintained at this time. Both are short-haired, tri-colored strains. Their availability was found to be extremely limited. Previous research has shown that these strains uniformly reject interstrain full-thickness skin grafts and that they differ at no less than 4 to 6 of the histocompatabililty loci which control graft rejection [18].

Strain 2 animals were obtained from NCI Laboratories (Bethesda, MD) and strain 13 animals were obtained from Crest Caviary (Mariposa, CA). Preliminary experiments were performed to verify that these strains met four prerequisites for use as a "bridge" animal model between earlier wound healing studies and current transplantation studies:

1. that these strains would be robust enough to withstand the cell-seeded analog procedure, which involves two periods of surgery under anesthesia — one to harvest cells and another to graft.

2. that normal wound healing in these strains is comparable to that observed in the Hartley strain.

3. that the cell-seeded ECM analog grafts would induce a response in these strains comparable to that seen in the Hartley strain.

4. that interstrain grafts are in fact uniformly rejected.

A test of criterion (4) was deemed necessary given the somewhat dilapidated state of U.S. guinea pig resources at the present time, the resultant possibility of nonuniform breeding standards, and the rather long interval of time since the graft rejection study cited above had

been performed. It was clear that a test of criterion (1) would be carried out *de facto* in the process of testing criteria (2) - (4).

The four criteria were tested as follows:

(a) The hardiness of the animals was tested as they were subjected to grafting procedures to test criteria (2) - (4).

(b) The healing response was tested with silicone control grafts. Four strain 2 and four strain 13 animals each had a 3 cm^2 full-thickness piece of skin surgically removed under anesthesia (see Grafting, surgery below). A thin (0.5mm) 3 cm^2 silicone sheet (Silastic, non-reinforced medical grade, Dow Corning, Midland, MI), comparable to the silicone component of the ECM analog, was sutured in place. The sheet functioned as an epidermis for the duration of the experiment. The experiment lasted until the wounds had closed by contraction and scar formation.

(c) Cell-seeded ECM analog response was tested by grafting four animals, two of strain 2 and two of strain 13, with 3 cm^2 cell-seeded grafts.

(d) Interstrain rejection was tested by exchanging full-thickness 3cm^2 skin grafts between strains.

7.3.3 Cell-seeded ECM Analog Preparation

Preparation of cell-seeded ECM analogs has been described in detail elsewhere [40]. A brief summary of the protocol is presented below:

The following procedures were carried out under asceptic conditions. ECM analog sheets were removed from the 70% isopropanol storage medium; 3 cm^2 grafts were cut and rinsed in phosphate buffered saline (PBS). Cells were harvested from biopsies obtained from the guinea pig dorsum under general anesthesia (see below, under Grafting). Biopsies were excised with a Goulian knife (Edward Weck and Co., Research Park, NC) to a depth of 0.006 inch with an area of approximately 3 cm^2. Hemostasis was achieved by blotting with sterile gauze, and the biopsy site was bandaged. The bandaging protocol was modified (see below) from the method of Orgill [40]. Biopsies were rinsed in sterile PBS and enzymatically digested to separate the epidermis from the dermis. Various digestion protocols were used including 2.5% trypsin at 37°C for 40 minutes, 0.25% trypsin at 4°C overnight, and 2.4 units/ml of dispase at 37°C for 30 minutes. The separated tissue was vortexed in cell culture medium supplemented with 10% fetal calf serum. In trypsin-separated tissue, only the dermis was vortexed. Both the epidermis and the dermis were vortexed when Dispase was used. The suspension was ltered through a single layer of cheesecloth and centrifuged to allow adjustment of cell density. The ECM analogs were blotted to remove retained moisture and 2.6 ml of cell suspension was pipetted into each 3 cm^2 graft. The grafts were placed in a customized, machined-lexan holder and gently centrifuged at 100 x g for 15 minutes.

7.3.4 Grafting of Cell-Seeded ECM Analogs and Control Skin Grafts

Grafting of ECM analogs, with and without seeded cells, as well as skin grafts, has been previously described in detail [40]. The grafting method of Orgill [40] was followed in outline. This method is briefly described and alterations are noted.

Animals were caged for at least one week after arrival from the supplier. They were fed a standard diet and housed individually or in pairs. The skin surface was prepared immediately

before taking epidermal biopsies for cell harvesting. The method of Orgill [40] was modified to further reduce chances of infection. After shaving with an electric clipper and chemically depilating (Nair, Carter Products, Irvine, CA), the skin surface was treated with surgical scrub for at least 30 seconds, and then rinsed with 70% ethanol or 70% isopropanol. Scrub and alcohol were applied four more times. The animal was then anesthetized. The grafting reported here was done under general anesthesia using Isoflurane as the inhalant. This gas was adopted because it seemed to avoid the severe, occasionally irreversible central nervous system depression observed with a previously used agent, Halothane.

If the grafting procedure involved ECM analogs seeded with epidermal cells then the cells were first harvested and the grafts prepared as described above. The animals were bandaged and allowed to recover from anesthesia in an incubator until the grafts were ready. A pre-operative dose of antibiotic (Keflin, Ely Lily and Co., Indianapolis, IN) was administered in preparation for grafting.

Once the ECM analog graft or one of the various control skin grafts was prepared, a 3 cm^2 wound bed was excised by cutting down to but not including the panniculus carnosus on the dorsum of the guinea pig. The graft was applied to this full-thickness skin wound and sutured in place with non-dissolvable nylon sutures (Ethilon, Johnson and Johnson, Somerville, NJ). The graft site was bandaged and, if a biopsy had been taken for cells, the biopsy site was rebandaged. The bandaging protocol was a modification of the method described by Orgill [40]. Biopsy sites were covered with petroleum-impregnated gauze (Xeroform, Cheesebrough-Ponds, Inc., Greenwich, CT). Graft sites were covered with a non-stick dressing (Telfa pad, Kendall, Boston, MA). The inner dressing(s) were wrapped with a single layer of Elastoplast (Beiersdorf, Inc., South Norwalk, CT). Extra gauze (Topper sponge, Johnson and Johnson, New Brunswick, NJ) was added beneath the Elastoplast to prevent excessive adherence to skin and hair. A short, rolled tube of Stockinette (Chaston, Dayville, CT) bandage material was then pulled over the animal's body, arms holes were cut, and the Stockinette was secured around the body by wrapping with tape (Elasticon and Zonas, Johnson and Johnson, New Brunswick, NJ). It was not necessary to apply any adhesive surfaces to the animal's body by this method. The animals were recovered on heat and returned to their cages.

7.3.5 Description of Grafts Applied in this Study

A summary description of the grafts applied in this study follows, including experimental rationale and a nomenclature which will be followed for the rest of this thesis. Each type of graft was assessed for rejection by gross observation and by a quantitative T cell assay, as described below. All grafts were 3cm^2.

Control grafts:

1. **allograft** Interstrain full-thickness skin grafts were transplanted to verify the inbred strain 2/strain 13 rejection model and to establish a strongest-response control.

2. **isograft** Full-thickness skin grafts were transplanted between animals of the same inbred strain. The isografts tested the genetic homogeneity of the strains and established the background level rejection response for the model.

3. **autograft** Full-thickness skin grafts were excised from an animal, rotated 180° and replaced (maintaining epidermal-dermal orientation). These grafts were intended to establish a

lowest-response control. Autografts were compared to isografts to assay for residual rejection between animals of the same strain.

4. **autocell ECM analogs** ECM analogs were seeded with cells obtained from a given animal and the seeded graft was grafted back onto the same animal. These grafts were intended as low-response controls to be compared with ECM analogs seeded with foreign cells.

5. **iso-allocell ECM analogs** ECM analogs were seeded with cells obtained from a given animal of the Hartley outbred strain and grafted onto another animal of the Hartley strain. Because these grafts are between animals of the same strain, they are technically cell isografts. However, because the Hartley strain is outbred, these guinea pigs are not nearly as closely related genetically as the animals of a true inbred strain, and these grafts should also be considered cell allografts. The designation iso-allocell was therefore adopted. These grafts were transplanted in order to provide a point of comparison with Orgill's earlier data [40].

6. **ECM analogs alone** ECM analogs containing no seeded cells were grafted. The response was measured to assess the contribution of the ECM analog alone to the response seen with cell-seeded ECM analogs. All ECM analog grafts, seeded and unseeded, were comprised of a CG matrix layer and a silicone layer, as described above.

7. **silicone alone** Grafts comprised solely of a silicone layer were applied to assess the rejection response to this material and to provide wound healing controls free of CG matrix.

8. **intact skin** The quantitative rejection assay described below was applied to intact skin to provide a zero-response control for the assay. Skin was taken from a guinea pig dorsum after shaving and applying depillatory and five applications of surgical scrub with alcohol rinses.

Test grafts:

9. **allocell ECM analogs** Experimental grafts consisted of ECM analogs seeded with cells of one strain (strain 2 or strain 13) and grafted onto an animal of the other strain. These grafts were designed to simulate, in a consistent, reproducible manner, grafting between immunologically unmatched humans. These grafts were used to test whether transplantation of epidermal cells across a histocompatibility barrier results in significant rejection.

7.3.6 T cell Assay

A quantitative assay was developed to measure the rejection response. This assay was based on a recently available monoclonal antibody specific for guinea pig T cells. T cells are known to be significant players in graft rejection [41], and it was decided that quantifying T cells in grafts would be a useful assay of rejection. The developed protocol was based on well-known immunohistochemical methods [42].

Briefly, the grafted animal was sacrificed between 10 and 20 days post-grafting, based on previous rodent studies of T cell response in graft rejection [41]. The graft area was excised from the guinea pig dorsum and a cross-sectional biopsy was removed. The biopsy was embedded (O.C.T. compound, Miles, Elkhart, IN) and frozen at $-70°C$. The frozen tissue blocks were

sectioned on a cryostat and thin sections were placed on histological slides. The sections were then incubated with the T cell antibody (mouse monoclonal, JRH Biosciences, Lenexa, KS), and unbound antibody was rinsed off. A secondary antibody was applied (Diagnostic Products Corp.) which recognized the first antibody and contained a linked peroxidase enzyme. Excess secondary antibody was rinsed off. A substrate was applied which produces a colored product upon reaction with the peroxidase enzyme. Cells with bound antibody were thereby stained. The stained tissue sections were preserved by applying mounting medium and a cover slip. Figure 15 summarizes the T cell localization process. Figure 16 describes the nature of the immunoperoxidase stain in detail.

In order to quantify the localized T cells a counting procedure was developed. A square 10 by 10 counting grid was used to count cells in a 400× microscope field (Optiphot, Nikon, Garden City, NY). Thirty counts were made of each tissue slice. Two tissue slices were counted per biopsy for a given graft type. All sixty counts were averaged to obtain a mean test score. Control sections were prepared for every biopsy by omitting the primary antibody. The control sections were used to assess non-specific binding of the secondary antibody. Sixty counts were also performed for the controls and an average was calculated. The control average was subtracted from the test average to calculate the specific signal for a given biopsy. All biopsies for a particular graft type were averaged to give a total mean count for each graft type. The counting procedure is described in Figure 17.

7.3.7 Wound Healing Analysis

Animals were rebandaged at regular intervals to assess the progress of the grafts. A qualitative assessment of graft rejection was sought by this method. Gross visual and occasionally tactile observations were recorded and the graft area was photographed. Observations included evidence of inflammation or necrosis, extent of epithelialization, degree of contraction, and evidence of ECM analog degradation.

The use of the modified bandaging protocol seemed to reduce the stress experienced by the animals during removal of old bandages and application of new ones. The process of rebandaging was nevertheless stressful and special efforts were successfully made to calm the animals. If this is not possible, a light dose of a sedative/analgesic such as buprenorphine (e.g. Buprenex, Reckitt-Colman Pharmaceutical Co., Richmond, VA.) is recommended.

Qualitative assessment of rejection was also obtained at time of sacrafice by harvesting biopsies for standard histological staining. Tissue sections were cut from the excised wound bed and fixed in Bouin's fixative. The tissue was paraffin-embedded and sectioned. Slides were prepared using trichrome as well as hematoxalyn and eosin staining. Slides were analyzed by light microscopy for evidence of rejection or tissue regeneration.

7.4 Results

7.4.1 T cell Staining

A number of different cell types were stained by the anti-T cell immunoperoxidase method. The significance of apparent shape differences revealed by the stain was tested by examining immunoperoxidase sections stained with an antibody against alpha-smooth muscle actin. The characteristic morphology of endothelial cells comprising capillary walls were clearly delineated by this method.

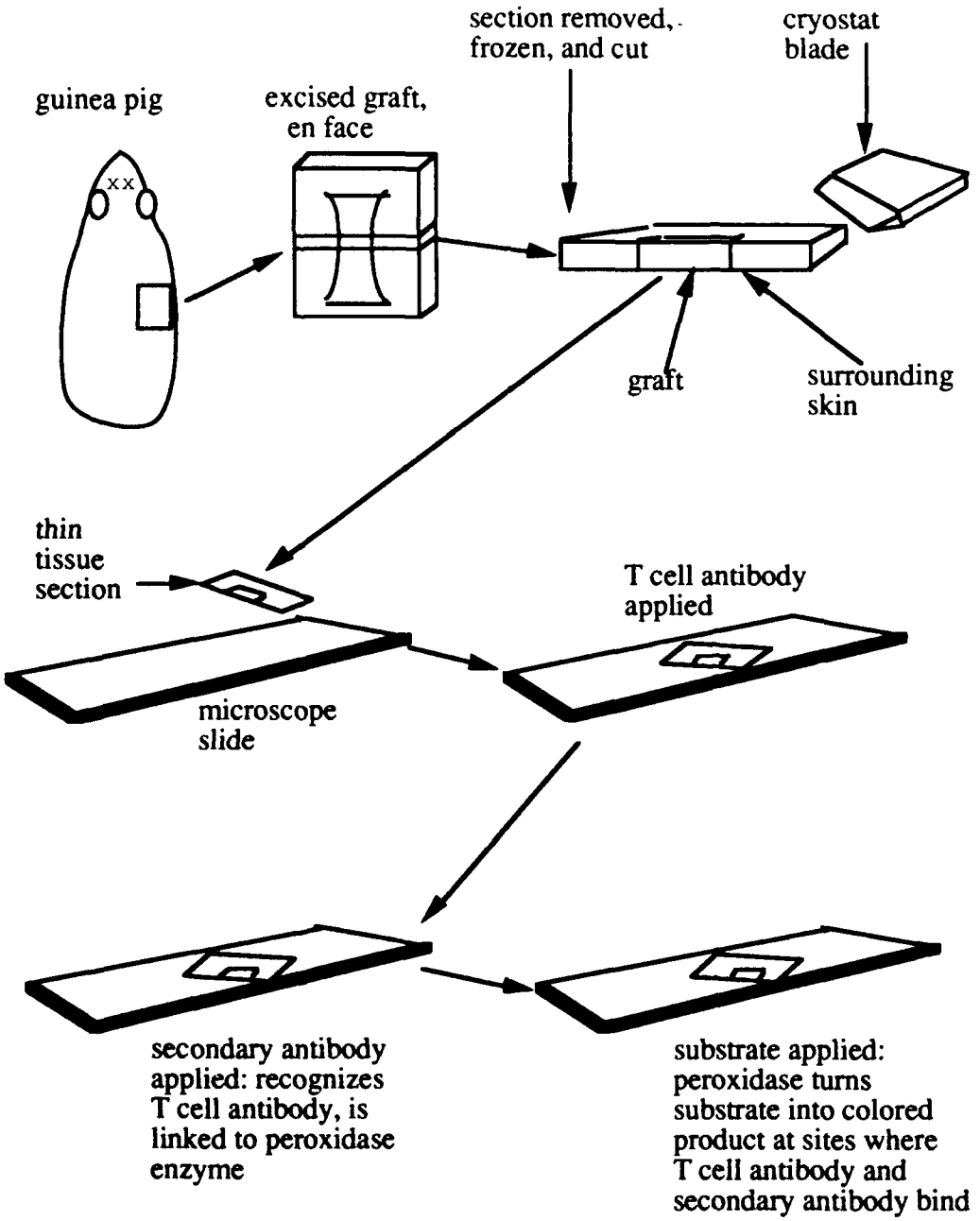

Figure 15: Localication of T cells in guinea pig grafts.

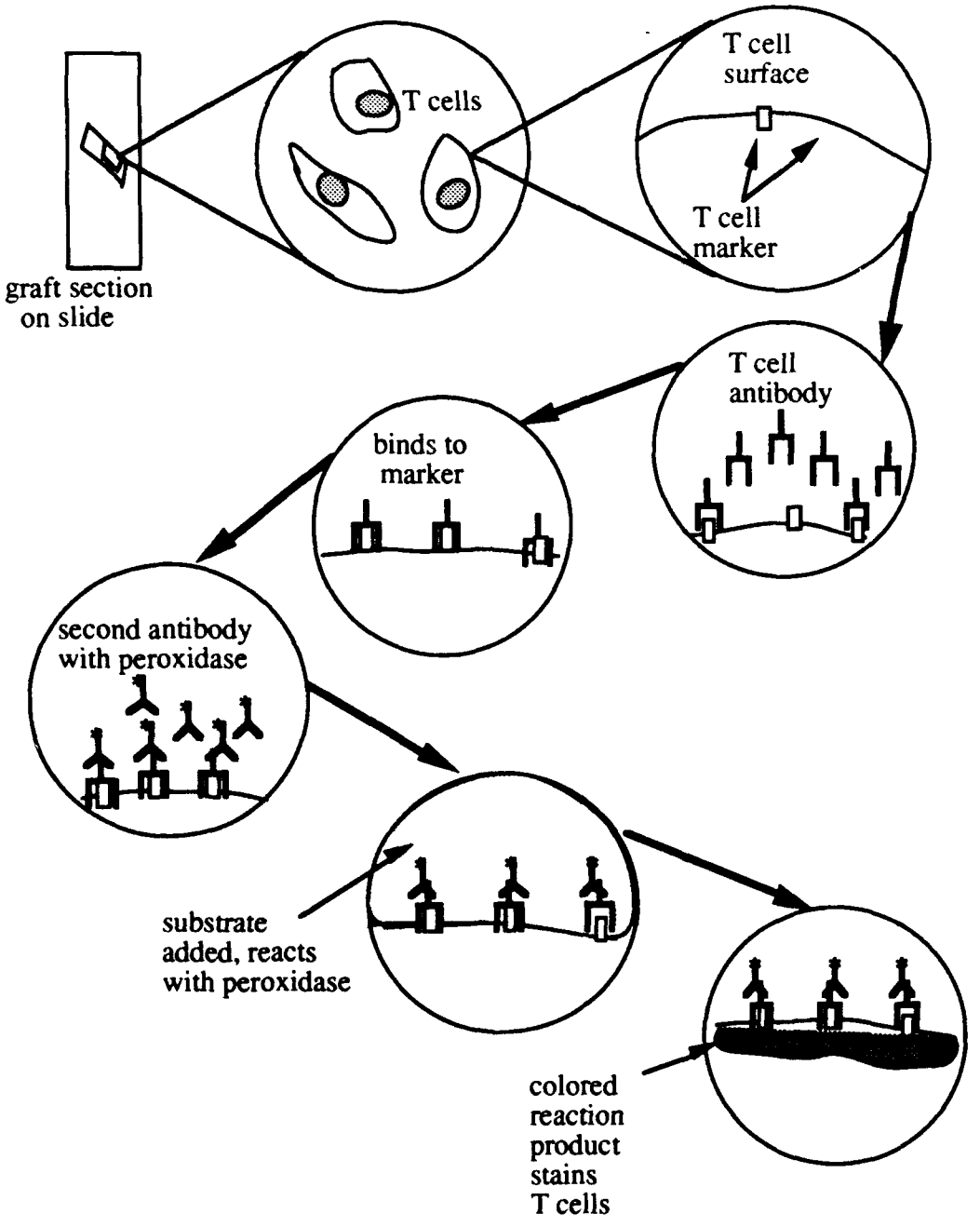

Figure 16: Immunoperoxidase method for visualizing localized T cells.

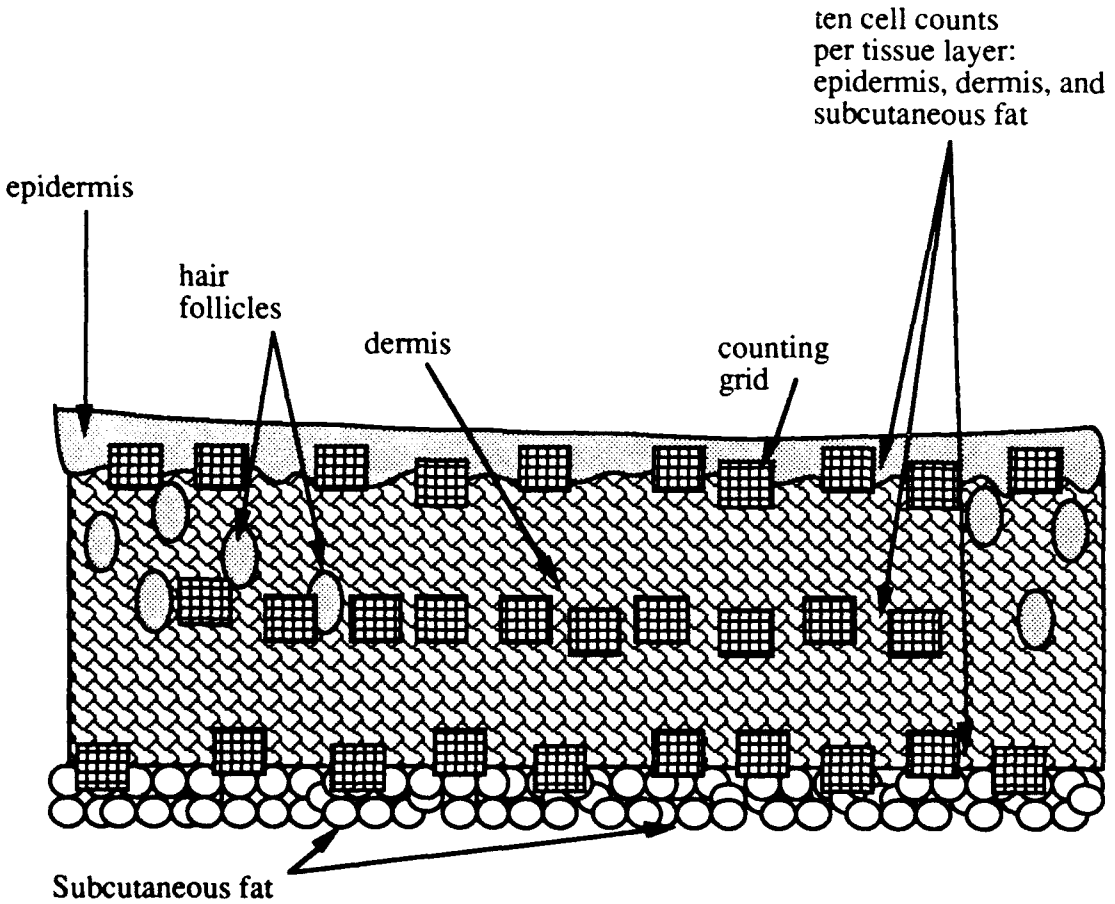

Figure 17: Counting stained cells in graft cross-sections. Each counting grid firgure represents a 10 × 10 grid field seen in the microscope eyepiece (400×). The counting field was scanned over each tissue slice and the number of cells observed in each grid field was recorded. Stained cells tended to cluster toward the top and/or bottom of the grafts. A pattern of counting ten grids along the top, middle, and bottom of the grafts was adhered to for all grafts. Two such sections were counted on each histology slide, each slide corresponding to one biopsy of a graft type. Control slides lacking T cell antibody were prepared from each biopsy. Control averages were subtracted from test averages to give an average specific response. Counts for all biopsies from each graft type were averaged to calculate a total mean response.

The following cell staining morphologies were consistently observed:

Type 1 Cells which displayed a large and irregular shroud of light stain around round to oval nuclei. Found in sections of all graft types. Variable location and abundance within grafts. See Figure 18A.

Type 2 Cells whose location (generally dermal) and shape (elongate) were characteristic of fibroblasts. These cells commonly displayed a small amount of light stain with an elongate distribution. The nuclei of these cells stained darkly with hematoxalyn counterstain and appeared variously thin, angular, and elongate depending on the plane of section through the cell. The nucleus was smaller than that seen in type 1 cells. Some type 2 cells were strongly stained and showed a more extensive shroud of stain around the nucleus, but the elongate distribution of stain remained. These darker-staining cells tended to occur in clusters. See Figure 18B.

Type 3 Cells characteristically residing in the wound border of ECM analog grafts and occasionally elsewhere. These cells showed very strong staining. The stain was dark and confined to an oval or somewhat irregular border around the nucleus. The nucleus often appeared to be two nuclei in the cryosections used for the T cell stain. However, examination of higher resolution trichrome and hematoxalyn and eosin (H&E) sections, in which the location of type 3 cells could be inferred, revealed only single nuclei. In addition, cells with the double nucleus morphology were often seen in large groups. This ruled out the possibility that this morphology arose from chance observations of cells undergoing mitosis. These cells most often occurred in groups at the graft edges but occasional single cells were also observed throughout the grafts. See Figure 18C.

Type 4 Cells typically associated with dense cellular infiltrates of infected and/or rejected grafts. Staining was intermediate in intensity between type 1 and type 3 and confined to a narrow rim around a round nucleus. See Figure 18D.

A preliminary correlation between type 1 – type 4 and known cell types is suggested in the Discussion.

For the purposes of the T cell assay, it was assumed that the stained cell population included T lymphocytes, macrophages, and other lymphocytes (see Discussion). This heterogeneous response was consistent and reproducible. The quantification of this response was taken to be a meaningful measure of rejection. Results of measuring the T cell response to control and test grafts are presented below. [Note that graft types (1) through (8) are considered control grafts with respect to the allocell ECM analog graft, the test graft. Under each graft type is a description of stained cells seen in test sections and control sections cut from biopsies of that graft type. Please refer to Materials and Methods for an explanation of graft nomenclature.]

7.4.2 Control Grafts

1. **Allografts**: Three allografts were biopsied, giving individual mean test counts of 32.47, 61.83, and 70.48, with corresponding mean control counts of 0.63, 1.62, and 5.35. Subtracting controls and averaging gave a total mean count of 52.39 with a standard deviation of 17.98 (Table 3, Figure 19).

   Biopsies were obtained at thirteen and nineteen days after grafting. Type 2 stained cells were abundantly distributed throughout the dermal region of the test biopsy sections.

A. Type 1 stain. Nuclei are round to oval; stain is light, widely-distributed. 700x.

B. Type 2 stain. Note elogate cell shape and stain distribution. 175x.

C. Type 3 Stain. Nuclei are dark with a double appearance. Stain is dense and close to nuclei. 700x.

D. H&E view of cell type which shows Type 4 stain (arrows). Note round, dark nuclei and thin cytoplasm. 700x.

Figure 18: Four consistently observed stained cell types. Stain types refer to the localized patterns of dark brown stain. All cell nuclei in *A*–*D* have stained purple (dark) with hematoxalyn. *D* shows the morphology of cells which have been observed to have type 4 staining, although this section has not been stained for T cells.

Table 3: **Individual average and total mean stained cell counts.**
The table contains individual entries in the form of averages from sixty counts per biopsy. Each entry corresponds to one biopsy of a certain graft type. The number entry is the result of subtracting the average control section count from the average test section count. Included are the results of the Kolmogorov-Smirnov goodness-of-fit test, expressed as percentage fit to a normal distribution.

	autograft	isograft	allograft	autocell ECM	isoallocell ECM	allocell ECM	ECM	silicone	intact skin
individual biopsy averages (test minus control)	7.72	4.40	31.83	3.98	8.10	6.62	7.73	26.35	2.05
	1.95	5.28	60.22	5.40	5.65	2.83	1.06	27.65	0.32
	2.73		65.13	4.23		17.82	10.95		
						3.86			
						11.98			
						20.48			
						32.30			
total mean	4.13	4.84	52.39	4.54	6.88	13.70	6.58	27.00	1.18
std. dev.	3.13	0.62	17.98	0.76	1.73	10.62	5.04	0.92	1.23
normal fit(%)	100.0	100.0	100.0	100.0	100.0	100.0	100.0	100.0	100.0

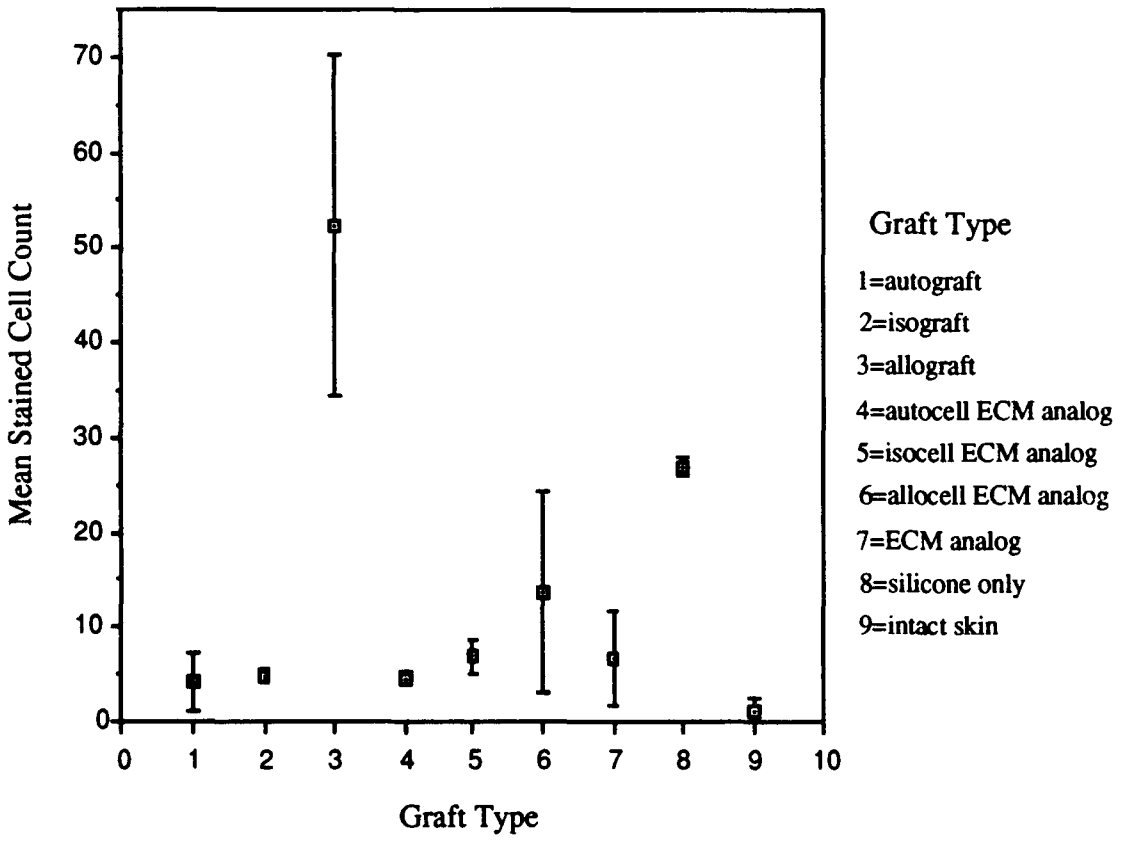

Figure 19: Mean stained cell counts for each graft type. Error bars give ± standard deviation.

The upper dermal zone contained many cavities, apparently the result of hair follicle degradation, and these contained many type 1 cells. This same zone also contained many prominently stained multinucleated giant cells which were clearly engaged in graft degradation. The degraded epidermal and upper dermal regions of these grafts contained by far the highest concentration of stained cells. All stained cell types were observed in this region. Clear examples of type 4 cells were not common. It was often difficult to decide whether cells which had a round nucleus and a fairly narrow rim of stained cytoplasm were small type 1 cells or large type 4 cells. Cells with type 2 elongate morphology but type 3 strong staining were common in clusters at the border between the grafts and surrounding normal tissue. These clusters contained type 3 cells as well. The adipose zone along the bottom of these grafts contained small numbers of types 1 and 2 cells.

Control sections contained strongly staining type 2 and type 3 cells in the same locations observed in test sections. A few type 3 and type 2 cells were observed in the adipose zone.

2. **Isografts**: Two isografts were biopsied, giving individual mean test counts of 4.50 and 5.33, with corresponding mean control counts of 0.10 and 0.05. Subtracting controls and averaging gave a total mean count of 4.84 with a standard deviation of 0.62 (Table 3, Figure 19).

   Test sections contained stained cells distributed along the top and bottom of the grafts in preference to the middle of the grafts. These were primarily type 1 cells, with a few type 2 cells. The superbasal epidermal zone was consistently vacuolized and stained cells often clustered in these regions. The morphology of these cells was difficult to determine because the stain tended to adhere irregularly to the vacuolized epidermal elements, but the cells were clearly of either type 1 or type 2 morphology. A prominent mass of stained cells occurred at the ends of the graft, where the graft edge is apposed to normal skin. These appeared to be primarily type 1 cells but some cells were relatively small and dark-staining suggesting type 3 or type 4.

   Control sections contained an occasional type 1 cell.

3. **Autografts**: Three autografts were biopsied, giving individual mean test counts of 7.72, 2.75, and 2.73, with corresponding mean control counts of 0, 0.8, and 0. Subtracting controls and averaging gave a total mean count of 3 with a standard deviation of 3.13 (Table 3, Figure 19).

   Test sections contained type 1 stained cells sparsely distributed throughout the graft. A few clusters of these cells occurred along the bottom of the graft (adipose zone). There was no obvious overall distribution in the grafts other than a slight tendency for these cells to occur in the adipose and epidermal zones. Considerably fewer type 2 stained cells were found. These occurred principally in the middle of the grafts (dermal zone) but also in the papillary dermis near the epidermis. A thin layer of intense stain was observed to overlie the graft epidermis. Close examination revealed a dense layer of cells and cell debris. The density of the layer precluded any morphological characterization of the constituent cells. This layer was apparently comprised principally of cells from the suprabasal layers of the epidermis. These layers displayed vacuolization and minor

degradation, and the resulting free cells and cell debris likely formed the stained layer. No type 3 or type 4 cells were seen in these grafts.

Control sections were largely bereft of staining cells. However, a few prominent concentrations of type 1 cells were seen in the adipose zone.

4. **Autocell ECM analog**: Three autocell ECM analogs were biopsied, giving individual mean test counts of 7.80, 10.48, and 4.62, with corresponding mean control counts of 3.82, 5.08, and 0.38. Subtracting controls and averaging gave a total mean count of 4.54 with a standard deviation of 0.76 (Table 3, Figure 19).

   Autocell ECM analogs biopsied between ten and twenty days post-grafting) showed a characteristic structure. The silicone layer had been removed from the graft by the time biopsies were taken. The uppermost layer of the graft consisted of either a maturing neoepidermis, in the case of a proliferative response by the seeded cells, or else a a dense cellular layer infiltrated by polymorphonuclear lymphocytes (PMNL's) and containing dead cells and degrading graft material, in the case of a nonproliferative response by the seeded cells. The middle layer of the graft consisted of a zone of matrix infiltrated by host mesenchymal cells and included donor seed cells during the first two weeks after grafting. After this time the seeded cells had either proliferated and migrated to the top of the graft to form a new epidermis or else they had died.

   All three autocell ECM analogs biopsies were obtained at eighteen days after grafting. One graft produced a neoepidermis by ten days, the other grafts failed to produce a neoepidermis. One of the latter maintained a healthy appearance until the biopsy was taken; the other showed signs of infection.

   Test sections contained many stained cells. Type 1 stained cells were seen spread throughout the grafts. Type 3 stained cells were also widespread but tended to occur in clusters. In the one graft containing neoepidermis, a line of type 3 cells was arranged along the border between the uppermost dermis and the neoepidermis. Type 3 cells also occurred in the middle of this graft and along the bottom edge of the graft. In the two grafts which lacked neoepidermis, there was a relative paucity of type 3 cells. Type 3 cells tended in this case to be most abundant along the bottom of the graft, in the adipose zone at the interface with the wound bed. Some type 2 cells were seen in the dermis of the normal skin adjacent to each of the grafts and occasionally in the remnant dermis in the wound bed or in the dense cellular zone at the bottom of the grafts. Type 4 cells may have occurred in association with type 3 cells but their identification was made difficult by the clusters of strongly staining type 3 cells.

   Control sections showed more type 3 stained cells than any othertype. The number of type 3 cells was less than that observed in the corresponding test sections. For example, the prominent line of type 3 cells under the neoepidermis described above was still obvious and strongly stained but showed fewer cells stained cells. In general, type 3 cells occurred most commonly in the adipose zone. A few type 1 and type 2 cells were seen there as well.

5. **Iso-allocell ECM analog**: Two iso-allo ECM analog grafts Stage were biopsied, giving individual mean test counts of 8.48 and 6.73, with corresponding mean control counts of 0.38 and 1.08. Subtracting controls and averaging gave a total mean count of 6.88 with a standard deviation of 1.73 (Table 3, Figure 19).

The pattern of stained cells observed for iso-allocell ECM analogs followed the pattern described above for allocell ECM analogs. However, the increase in type 4 cells could not be documented within the T cell assay time frame since only two biopsies were taken, both ten days after grafting. Examination of two biopsies taken twenty-three days after grafting, beyond the T cell assay time frame, indicated that more type 4 cells were present at this point.

The day ten biopsies showed the characteristic type 3 stained cell distribution along the epidermal zone of the graft, with pods of types 2 and 3 cells at the graft edges. These cells persisted in smaller numbers in the control sections. The rest of the graft area, through the dermal zone and down to the base of the graft at the adipose layer showed types 1, 2, and 3 cells in the test sections. One day ten biopsy displayed neoepidermis and few signs of graft degradation. A very few type 4 cells were observed in the epidermal zone of this section. The other day ten biopsy showed clear signs of graft degradation. The epidermal zone consisted of a skeletonized network of extracellular matrix and dead cells. Type 3 cells were distributed across this zone. Types 1 and 2 cells lined the various small cavities that were forming at the bottom of the graft. Type 4 cells could be observed infiltrating the graft in this area via blood vessels.

6. **ECM analog alone**: Three ECM analog grafts were biopsied, giving individual mean test counts of 7.73, 1.08, and 11.25, with corresponding mean control counts of 0, 0.02, and 0.3. Subtracting controls and averaging gave a total mean count of 6.58 with a standard deviation of 5.04 (Table 3, Figure 19).

   The appearance of ECM analog grafts varied considerably from six days after grafting (earliest sample) to nineteen days post-grafting (latest sample). The early graft showed extensive strands of free ECM analog between remnant silicone above and remnant dermis in the wound bed below. Between the remnant dermis and the bottom surface of the ECM analog graft was a layer of ECM analog which had been populated by cells (Table 3, Figure 19). The entire graft area showed considerable staining. Type 3 and 4 cells populated the ECM analog area, while the remnant dermis and infiltrated matrix contained type 1 and 2 cells. Some strands of dense heavily staining material were observed to overlie the epidermis of the normal skin at the would edge, as described above for autografts. No other clustering of cells at the graft edge was observed.

   The same overall distribution of cells was observed at nineteen days after grafting. At this point the ECM analog had become almost entirely infiltrated with cells; only a few strands of free ECM analog were observed at the top of the graft immediately beneath the remnant silicone. Type 3 and 4 cells continued to be visible in this thin free matrix zone while type 1 and a few type 2 cells predominated in the cell-infiltrated matrix zone. It was inferred from the way the silicone remnants were scattered from the ECM analog that the free matrix strand zone may be an artifact of sectioning, in which the upper layers of the graft are pulled away from the lower ones by the action of the cryostat cutting blade. A layer of stained cells was often visible along the edge of the graft which had been in contact with the silicone layer. Clusters of staining cells were also seen in association with remnant silicone bits. The association between stained cells and silicone, while clear in places, was not uniform; silicone remnants with no associated stained cells or with a density of stained cells which was comparable to that seen in the middle of the graft were also common.

No staining was observed in control sections. All layers of the graft, including remnant silicone pieces, were free of stained cells.

7. **Silicone alone**: Two silicone control wounds were biopsied, giving individual mean test counts of 27.45 and 28.58, with corresponding mean control counts of 1.10 and 0.93. Subtracting controls and averaging gave a total mean count of 27.00 with a standard deviation of 0.92 (Table 3, Figure 19). Both silicone controls were biopsied nine days after grafting. The histological sections revealed a dense, cellular layer of granulation tissue between the silicone and the wound bed.

   Test sections showed abundant staining. Type 2 cells were seen throughout the granulation tissue layer. Together with type 1 cells they lined cavities which had formed in the lower part of the granulation tissue. Strongly staining type 2 cells were found together with all other stained cell types in the epidermis and papillary dermis at the wound edge. Types 3 and 4 cells were far less common than types 1 and 2. Pods of type 1 cells occurred throughout the granulation tissue. Some of these clusters appeared to be associated with granulation tissue degradation. Heavily stained multinucleated giant cells were also seen. The lower granulation tissue contained many cavities with associated stained cells. The uppermost layer of the granulation tissue, which had been in contact with the silicone, was capped by a monolayer of stained cells of indeterminate morphology.

   Staining of these cells was strong, but the layer was too thin and dense to allow further characterization. Staining of granulation tissue from silicone grafts was roughly similar to that observed in allografts. Type 2 cells were widespread, pods of type 1 cells were common, and tissue degradation in association with stained cells was common. The silicone sections differed from the allografts in that the latter showed prominent degradation and stained cells in the upper layer of the grafted area rather than at the wound bed interface as seen in the silicone controls .

   Control sections contained small, infrequent cluster of type 3 cells and a small number of type 2 cells in the dermis of the normal skin adjacent to the granulation tissue. A few type 2 cells were also seen in the adipose zone.

8. **Intact skin**: One site was biopsied on a single animal. For the test sections, a separate staining was carried out for each of two different tissue preparations from the same biopsy. A single control slide was stained. Individual mean test counts were 2.18 and 0.45, with a mean control count of 0.13. Subtracting the control and averaging gave a total mean count of 1.18 with a standard deviation of 1.22 (Table 3, Figure 19).

   Sparse type 1 stained cells were observed throughout the test full-thickness skin sections. About five times as many stained cells were seen in the epidermal-papillary dermis area as compared to the the reticular dermis and the adipose zone. There was a distinct concentration of stained cells along the uppermost edge of the skin sections, i.e. just beneath the surface which had been subjected to the antibacterial treatment. No other clustering or concentration of cells was evident elsewhere in the sections.

   Occasional type 1 stained cells were observed in the control section. There was no discernable pattern of distribution for these very widely separated cells. Stain was generally pale, often orange rather than the red expected for the AEC immunoperoxidase substrate. The stain was often not clearly associated with cell nuclei.

It was noted that the histological morphology of the intact skin sections was abnormal; all superbasal epidermal elements were absent. Because the tissue was biopsied and fixed immediately after application of depilating agent, surgical scrub, and alcohol, the altered morphology was inferred to derive from this treatment. This condition could have affected the T cell count: any cells which existed in the epidermis above the basal layer and which would have stained were lost from the counting procedure. Since T cells do not reside in normal epidermis [43], this effect did not likely have a great effect on the measured value for T cell level in intact skin.

7.4.3 Test Grafts

Allocell ECM analog: Seven allocell ECM analogs were biopsied, giving individual mean test counts of 12.68, 7.95, 18.60, 5.95, 12.70, 35.43, and 44.15, with corresponding mean control counts of 6.07, 5.12, 0.78, 2.08, 0.72, 14.95, and 11.85. Subtracting controls and averaging gave a total mean count of 13.7 with a standard deviation of 10.62 (Table 3, Figure 19).

ECM analog grafts seeded with cells crossed between guinea pig strains showed the same morphological characteristics described above for cell-seeded autografts. The seeded cells either proliferated or failed to proliferate within the first two weeks. After this time the graft was either covered with a neoepidermis or remained unepithelialized, being covered instead by a thin, dense zone of dead cells and extracellular matrix. Such grafts eventually become epithelialized, as shown by allocell ECM analogs which were allowed to progress beyond the T cell assay time frame.

A clear difference existed between staining of grafts of autocell and allocell ECM analogs: Allocell ECM analog grafts contained type 4 cells in test sections. Control sections lacked type 4 cells. Type 4 cells occurred in the upper, epidermal regions of the grafts among the cellular and matrix debris zone during the seeded cell proliferative phase, at the graft edges near the normal skin, and along the bottom of the grafts in the adipose zone (Figures 20 and 21). The number of type 4 cells increased with time: occasional type 4 cells were seen in the debris zone and adipose zone nine days after grafting; by twenty-two days after grafting type 4 cells could be seen in the border region between the graft and normal tissue and small pockets of type 4 cells were visible in the adipose zone.

Other stained cell types occurred with a distribution which mimicked autocell ECM analogs. Type 3 cells were the most prominent type; these were found in both test and control sections with identical distributions except that the control sections contained fewer of these stained cells. As with autocell ECM analogs, the type 3 cells tended to occur in clusters irregularly distributed throughout the graft. A consistent feature of biopsies taken after the seeded cell proliferative phase was a cluster of types 3 and 2 cells in the epidermal region at the border between graft and normal tissue. Type 1 cells were common in the biopsy taken at nine days after grafting, during the seeded cell proliferative phase, and more rare in the biopsies taken at fourteen and twenty-two days after grafting, when the proliferative phase had subsided.

7.4.4 Statistical Analysis of Staining Levels

Statistical significance of the T cell raw data was assessed using the t test and a Statgraphics (C sign) computer program (Statistical Graphics Corporation, 1986). The T cell counts of the biopsies from each graft type were tested for significance of fit to a normal distribution, using the Kolmogorov-Smirnov method (see Discussion). All data sets fit a normal distribution by

Figure 20: T cell stain of autocell ECM analog (day 18). A dense cellularlayer (large arrow) separates epidermis (ED) from dermis (D). Type 3 cells occur in this layer (small arrow). Types 1 and 3 cells stain elsewhere (small arrow). 175×.

Figure 21: T cell stain of allocell ECM analog (day 9). Types 1, 3, and 4 cells occur in the debris zone (arrow) above the neoepidermis (NE). Type 1 is seen in the NE, types 1 and 3 in the dermal area (D). 175×.

Table 4: **Significance testing of stained cell count comparisons.**
The first column summarized the results of the Two-Sample Analysis for significant difference between the variances of the compared data sets. Passing the comparable variance test is a prerequisite to employing the *t* test. The second column summarizes the results of the *t* test. The last two columns report the Normal Means calculated sample size for 95% confidence in claiming a difference between data sets and the actual sample size.

Graft Comparison	Passes Comparable Variance Prereq.	*t* Test Prediction: Sig. Dif. P = 0.05	Normal Means Minimum Sample	Actual Sample Size
allograft / autograft	yes	yes	2	6
allograft / isograft	yes	yes	2	5
allograft / allocell ECM analog	yes	yes[a]	3	10
autograft / allocell ECM analog	yes	no	13	10
allocell ECM analog / autocell ECM analog	no	no [b]	15	10
autograft / autocell ECM analog	yes	no	614	6
ECM / silicone	yes	no	1	5

[a]Passes test for P = 0.01
[b]Fails equal variance prerequisite for *t* test but shows no statistical difference by Statgraphics Two-Sample Unequal Variance test.

this analysis. The Kolmogorov-Smirnov analysis is reported as a goodness-of-fit in percent; 100% is perfect fit. The mean T cell count for each graft type and the associated standard deviation were then calculated. These results are summarized in Table 3.

Data sets for each graft type were compared for significant differences. To confirm the validity of *t* test application to this data, the Two-Sample Analysis function of the Statgraphics program (see Discussion) was used to verify comparable standard deviations for the pairs of compared data sets. All graft type comparisons were suitable for *t* test analysis by this criterion with the exception of allocell ECM analog versus autocell ECM analog. This comparison was carried out using the Two-Sample Analysis for Unequal Variances function of the Statgraphics program. The balance of the comparisons was carried out using the *t* test for 95% confidence level (p = 0.05). The results are reported in pairwise quantitative comparison graphical form in Figures 22–28. A summary of the comparisons is included in Table 4.

A sample size analysis was performed for each comparison using the Normal Means function of the Statgraphics program (see Discussion). The results of this analysis indicated that a sufficient number of animals had been biopsied in each data set in order to perform statistically significant comparisons between the data sets. The output of this analysis and the actual number of biopsies taken are given in Table 4.

T cell staining summary: Grafts of ECM analog, allocell ECM analog, autocell ECM analog, autografts, isografts, and intact skin all showed a low level of stained cells that did not vary significantly from group to group (Table 3, Figure 19). In contrast to this background level of staining, allografts showed a high level of stained cells, significantly higher than any

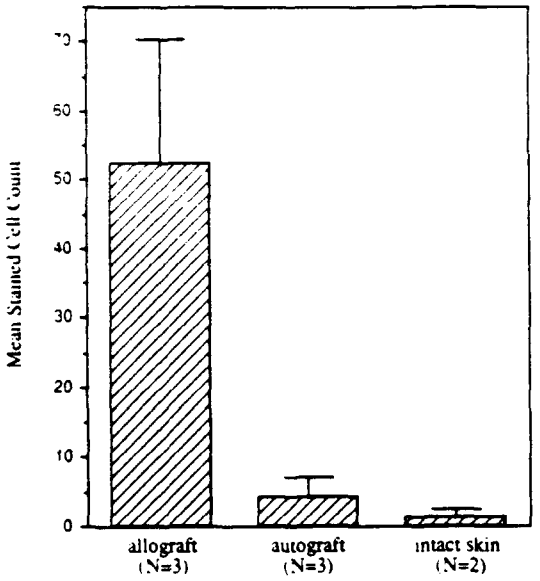

Figure 22: Mean stained cell response to allograft and autograft. The latter is significantly smaller than the former (p = 0.05). Intact skin for comparison.

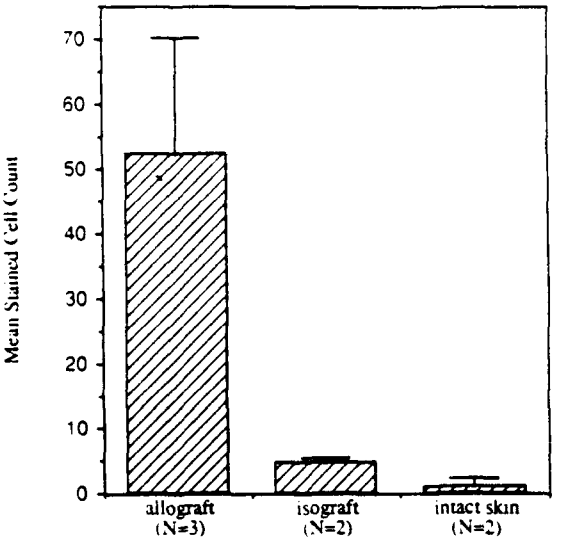

Figure 23: Mean stained cell response to allograft and isograft. The latter is significantly smaller than the former (p = 0.05). Intact skin for comparison.

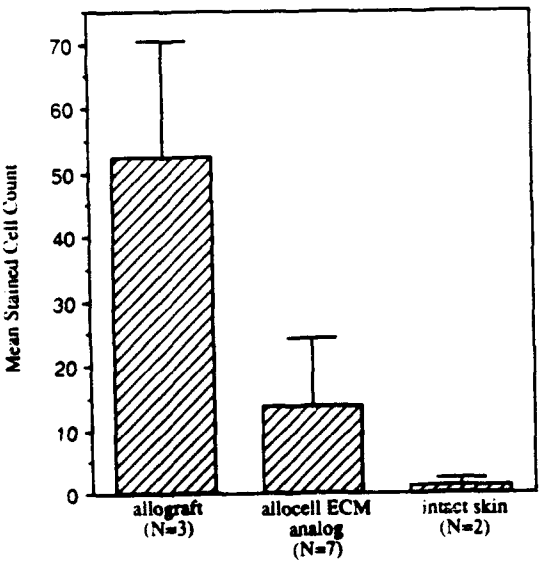

Figure 24: Mean stained cell response to allograft and allocell ECM analog (Foreign cells seeded in ECM analog). The latter is significantly smaller than the former (p = 0.05). Intact skin for comparison.

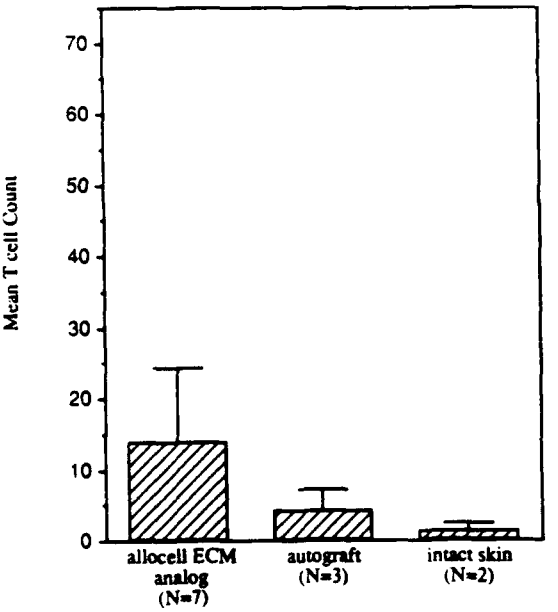

Figure 25: Mean stained cell response to allocell ECM analog and autograft. The two do not differ significantly (p = 0.05). Intact skin for comparison.

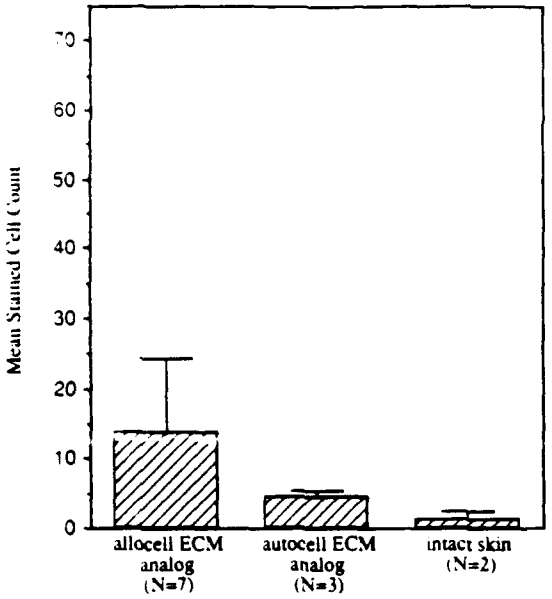

Figure 26: Mean stained cell response to allocell and autocell ECM analog. There is no significant difference between these grafts ($p = 0.05$). Intact skin for comparison.

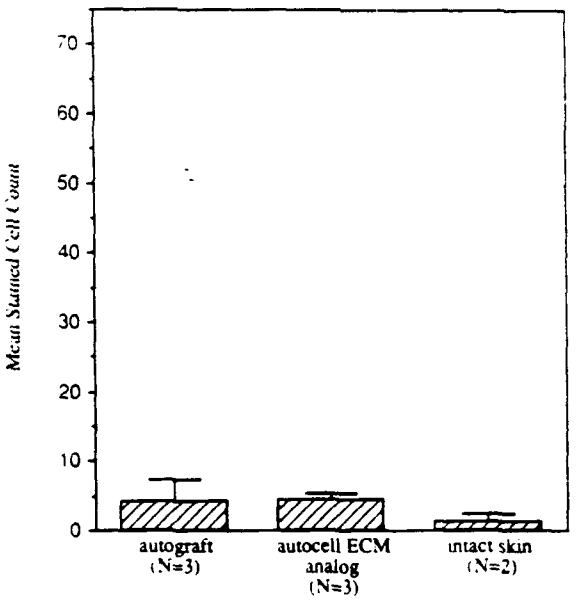

Figure 27: Mean stained cell response to autograft and autocell ECM analog. There is no significant difference between these grafts ($p = 0.05$). Intact skin for comparison.

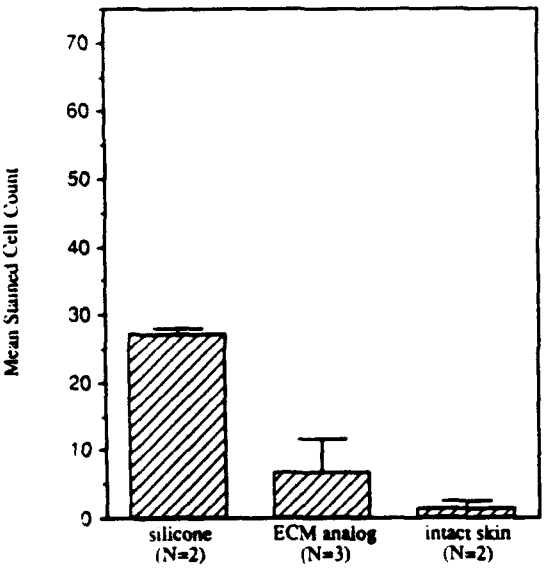

Figure 28: Mean stained cell response for silicone and ECM analog. Silicone response is significantly greater than ECM analog response ($p = 0.05$). Intact skin for comparison.

other graft type. Allocell ECM analogs showed a much lower level of stained cells than did allografts. Further, the allocell ECM analogs did not differ significantly from the background signal obtained with unrejected grafts. Silicone alone showed a significantly higher response than any other graft type except allografts. Figures 22–28 summarize these results in graphical form.

7.4.5 Wound Healing: Gross Observation

1. **Isografts** (between animals of the same strain) showed perfect take, with no signs of rejection through the 27 day extent of the experiment.

2. **Allografts** between 2 animals, each of a different strain, showed uniform rejection. By 8 days after grafting, the graft had reddened, and the epithelium was sloughing off. By 13 days after grafting, the graft was obviously necrotic, displaying extensive pus and degraded tissue.

3. **Autocell ECM analog grafts**: Autocell ECM analogs controls were grafted on Hartley outbred strain guinea pigs. (The grafts were prepared by seeding an ECM analog with disaggregated uncultured cells that were extracted from the animal that was eventually grafted.) These grafts served to link the present study to previous work in this laboratory [40]. The Hartley grafts controlled for any changes in experimental conditions which could have occurred since the previous work was done. Three gross patterns of wound healing were observed:

   (a) Strong seeded epidermal cell proliferation, stable re-epithelialization before 20 days post grafting, significant wound contraction (to approximately 20% of original wound area) without linear scar formation, re-expansion to approximately 50% original wound area by approximately 110 days post-grafting (see Figure 29).

   (b) Weak or undetectable seeded cell proliferation, re-epithelialization unstable or absent before 20 days post-grafting, wound continues unepithelialized until approximately 60 days post-grafting, wound closure by wound edge migration with a resulting closed wound that is approximately 10% to 20% of its original area, reexpansion to approximately 25% to 50% original area by approximately 110 days post-grafting.

   (c) Same characteristics as pattern 2, except there is no reexpansion and a linear scar results sometime after approximately 60 days post-grafting.

   The short-term behavior of autocell ECM analogs on Strain 2 and Strain 13 guinea pigs was qualitatively identical to previously reported results for Hartley guinea pigs [40]. Three of the four grafts showed significant seeded cell proliferation. The experiment was not continued long enough to verify wound re-expansion as seen on Hartley autocell ECM analogs after approximately 60 days post-grafting. The one graft which was maintained until 68 days post-grafting has become a linear scar. Another animal which was sacrificed on day 42 had also formed a linear scar.

4. **Allocell ECM analogs**: (Prepared by seeding an ECM analog with uncultured, disaggregated epidermal cells from Strain 13 and grafting onto Strain 2 animals.) Of sixteen allocell ECM analogs grafted, two animals died either during or shortly after the grafting procedure due to anesthesia complications. Of the remaining fourteen animals, ten were

sacrificed for T cell data; the remaining four animals were maintained for 102 days to assess the long term response to these grafts.

Two of the fourteen allocell ECM analogs showed a clearly abnormal response in comparison with the autocell ECM analog response. The grafts were degraded by twelve days post-grafting, with large amounts of ECM analog sloughing off the wound bed. The area around the grafts displayed significant full-thickness lesions where patches of skin were spontaneously degrading. These animals were sacrificed immediately and histologies were taken.

Twelve of the fourteen allocell ECM analogs appeared grossly identical to autocell ECM analogs. The silicone layer was nonadherent by ten or twelve days post-grafting. A vascularized bed of tissue was revealed when the silicone was removed. Six of the twelve grafts showed seeded cell proliferation.

The progress of four of these grafts was followed for 102 days:

(a) Graft 91U1 was re-epithelialized by fifteen to twenty days after grafting. This neoepidermis proved unstable and subsequently reopened by day 40. By day 75 the wound had closed permanently by wound-edge migration. On the day of sacrifice, at 102 days post-grafting, the wound was 22% of its original area. A linear scar at this point would have an area approximately 5% of its original area (see Figure 30).

(b) Graft 91U2 was never completely epithelialized until wound edge migration accomplished the task by day 65. By day 102 at sacrifice, the wound was 22% of its original area and clearly differed from a linear scar.

(c) Graft 91U3 closed to a linear scar by 40 to 45 days post-grafting. This state did not change by time of sacrifice at day 102.

(d) Graft 91U4 closed via wound-edge migration by day 55 to 9% of its original area. By day 102 sacrifice the graft was a nearly-linear scar.

5. **Silicone sheet**: Wound contraction observations of full-thickness wounds covered with silicone sheet sutured in place showed a variable time of contraction initiation. However, a linear scar was found to result in both strains by about 50 days post-grafting. The overall wound healing response, as assessed by this wound contraction assay, was comparable to that seen in previous studies [40].

7.4.6 Wound Healing: Histological Observation

Histological sections of allocell ECM analogs showed three broad phases of wound healing:

1. Seeded cell proliferative phase: Epidermal cells were seen to erupt from the middle of the graft, streaming and merging into a layer at the top (silicone side) of the graft. Remnant ECM analog pore channel walls seemed to guide the cells in this process. By as early as day 9, the epidermal cells had formed a confluent, stratified epithelial layer . Abundant spherical clusters of epidermal cells populated the lower and middle regions of the graft. These appeared to be rising to the surface of the graft and were clearly in the process of merging with other clusters and streamers of seeded cells. The top region of the graft was comprised of a thick layer of dead epidermal cells, extracellular matrix and keratin debris,

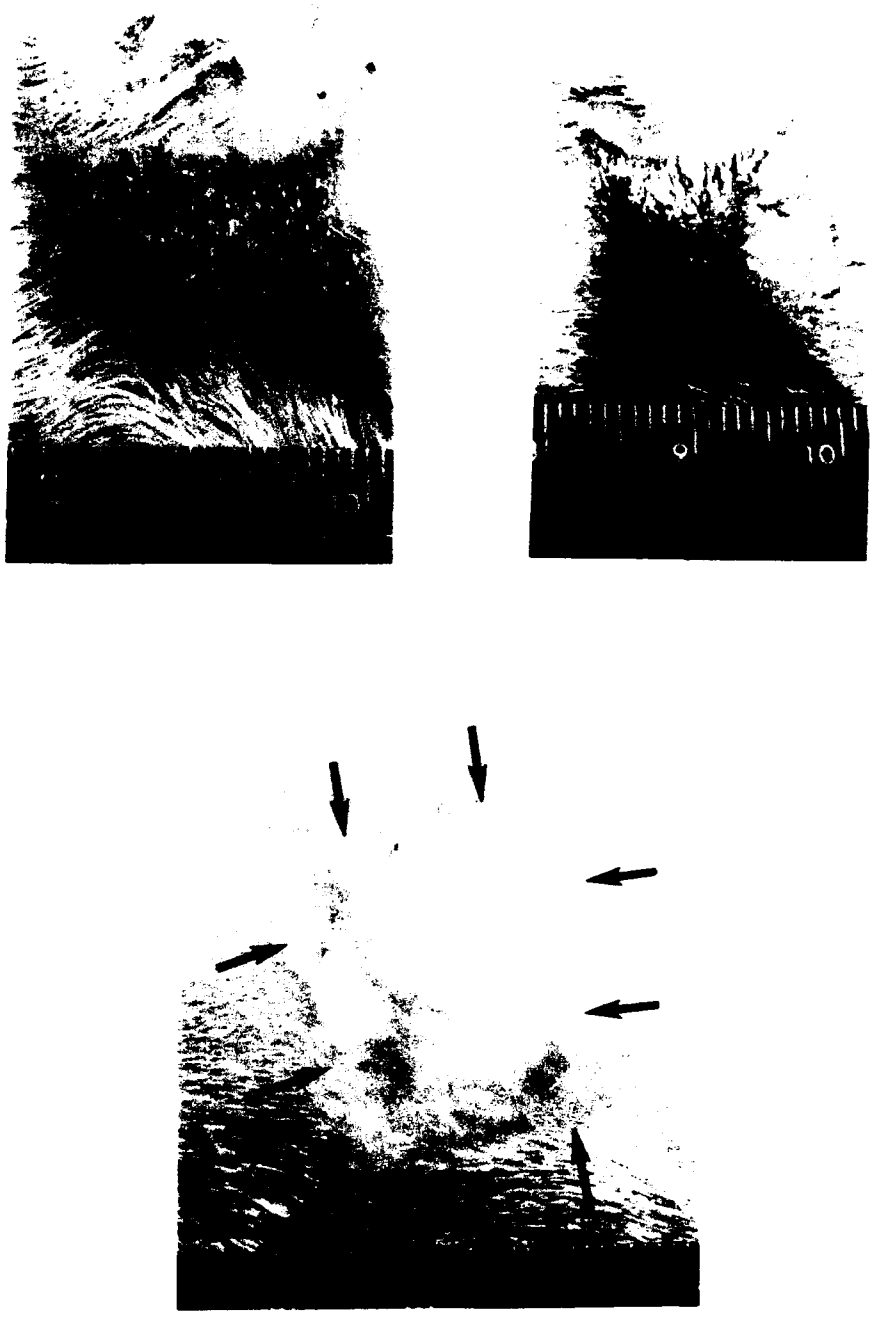

Figure 29: Autocell ECM analog graft on Hartley guinea pig; proliferation and re-expansion response. *Top left*: Day 17, during seeded cell proliferative phase. Note keratin pearls emerging from the graft (arrows). *Top right*: Day 24, vigorous contraction, wound is epithelialized. *Bottom*: Day 122, wound has expanded to occupy approximately 50% of its original area. Newly synthesized skin (arrows) has no hair or adenexa.

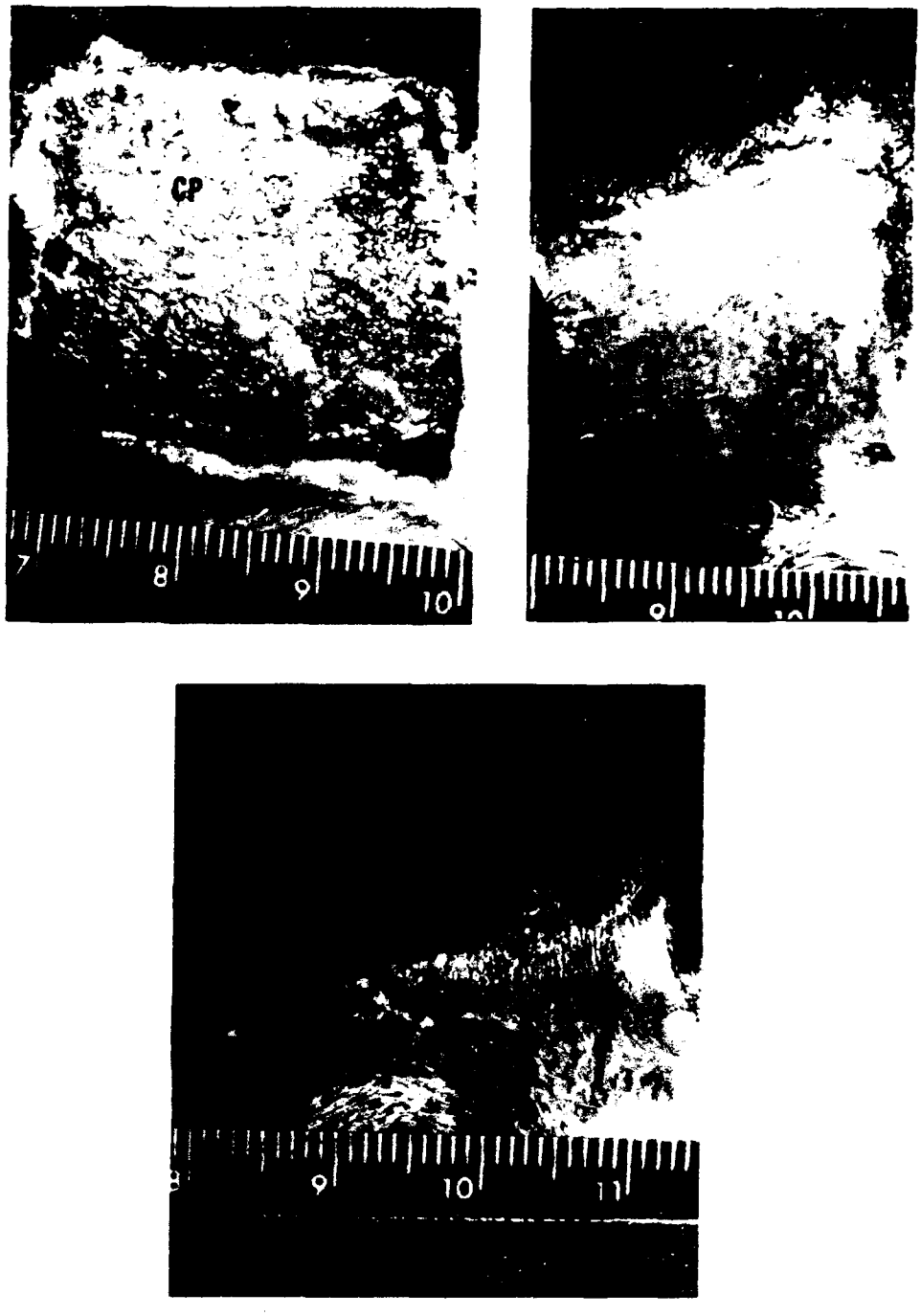

Figure 30: Allocell ECM analog on Strain 2 guinea pig. *Top left*: Day 10, seeded cell proliferation (CP) lightens color of graft. *Top right*: Day 22, graft has thin epithelial covering; thicker migrating epidermis is indicated (arrow). *Bottom*: Day 102, contraction has reduced wound area to 22% original; scar would be 5% original area. Arrows show wound edge.

and abundant infiltrating polymorphonuclear lymphocytes (PMNL's). Most of the graft was degraded as judged by the paucity of blue remnants in the trichrome sections, and by the numerous small blue remnants in the upper debris layer. Cells with a fibroblastic morphology were beginning to invade the bottom of the graft.

2. Post-proliferative, vigorous contraction phase: The dermal region of the grafts displayed an infiltrate of fibroblastic cells. A few grafts displayed a stratified neoepidermis. Other grafts displayed either a remnant poorly organized zone of PMNL's and necrotic tissue in the epidermal region of the graft or else a dense zone of granulation tissue.

3. Post-contraction, remodeling phase: The graft dermal region was more sparsely populated with fibroblastic cells, as compared to the contraction phase. Dermal morphology varied from scar-like, with dense parallel bundles of collagen fibers spanning a narrow, contracted wound, to dermal-like, with thick, wavy, random bundles of collagen spanning wide areas relative to a linear scar.

7.5 Discussion

Results are discussed in two categories: Quantitative and Qualitative.

7.5.1 Quantitative Results: T cell Assay

The goal of the T cell assay was to determine whether a response to foreign tissue could be quantified in a consistent, reproducible way. Rejection levels for allocell ECM analog grafts and all relevant controls could then be compared. This analysis would determine whether foreign epidermal cells are significantly less immunogenic than foreign skin. An affirmative answer would indicate a dermal locus for skin immunogenicity. A positive result would also indicate that allocell ECM analogs could have clinical use in skin replacement therapy.

The validity of the assay hinges on whether the immunoperoxidase method is capable of labelling a rejection response. The validity also hinges on whether the study produced enough meaningful data points to allow use of the standard methods of analysis employed here. Each of these points is considered below.

(a) **Immunoperoxidase Method.** Healing of wounds is an extremely dynamic process. High levels of both tissue degradation and tissue synthesis are found in a healing wound. Full-thickness skin wounds are infiltrated with many cells of different types in order to accomplish the healing [44]. This happens whether or not the wound is grafted and whether or not the grafting provokes a rejection response. Some elevated population of cells will appear in any of these cases in order to destroy pathogens invading the wound, remove debris, close the wound, and remodel the tissue.

Infection control and debris removal are activities which are known to predominate during the time frame chosen for the T cell assay [44]. These activities are performed by two major cell types, macrophages and lymphocytes. The process is very complex. It involves signalling between these cell types, as well as signals exchanged with other cell types. In a graft which is not being rejected, a normal wound healing response would be expected, one in which specialized cells of the immune system

would not be recruited. Warding off generic bacterial invaders and cleaning up debris can be accomplished by the macrophages and generic lymphocytes known as polymorphonuclear lymphocytes (PMNL's). When the wound is challenged with a completely foreign tissue, a rejection response occurs. This response involves more specialized immune cells, including T lymphocytes (T cells) [41].

It was expected that the immunohistochemical T cell assay would stain not only T cells but cell of other types as well. Macrophages and lymphocytes possess receptors (Fc receptors) for the constant region of immunoglobulin (antibody) molecules [42, 45]. Both the primary (anti-T cell) and secondary (anti-primary) antibodies would be expected to bind non-specifically to these receptors on the macrophages and lymphocytes, thereby staining them via the peroxidase assay.

It was clear upon examination of the preliminary results of the T cell assay that cells other than T lymphocytes had stained. By light microscope observations of the histology sections it was possible to identify macrophages and lymphocytes, including PMNL's and T cells. This was done on a morphological basis by reference to an histological atlas [43]. Figure 18D demonstrates that such morphological comparisons are possible. It should also be clear from this micrograph that attempting to quantify a certain cell type in a tissue section by shape alone would be an impractical task. It was for this reason that a staining assay was developed.

An analysis, based solely on knowledge of the non-specific macrophage and lymphocyte binding and on cell morphology, suggests the following taxonomy:

Type 1 cells included macrophages and lymphocytes. The type 1 large rounded nucleus and large irregular cytoplasm indicated by the staining were consistent with a macrophage morphology. Multinucleated giant cells, comprised of fused macrophages, were observed forming by the aggregation of type 1 cells. The multinucleated giant cells, once formed, displayed a type 1 staining morphology. Some type 1 stained cells were clearly PMNL's given the shape of their nuclei as revealed by the hematoxalyn counterstain. Some type 1 cells may be T lymphocytes. In degrading grafts which contained cavities apparently filled with type 1 cells, it was often difficult to differentiate between type 1 cells with a relatively thin border of stain and type 4 cells with a relatively large border of stain. In addition, grafts whose test sections showed many type 1 cells often showed very few type 1 cells in the corresponding control section.

Type 2 cells were difficult to identify based on known characteristics of skin cells. These cells appeared to be fibroblasts, but fibroblasts would not be expected to stain. Apparently, these cells are macrophages or lymphocytes which have adopted a particular morphology in order to negotiate the matrix-rich environment in which they are commonly seen. The association of type 2 with type 1 cells in cavities within degrading grafts also suggests a macrophage or lymphocyte.

Type 3 cells were histiocytes (fixed-location macrophages), based on previous reports of staining of these cells [45]. The association of these cells with the artificial skin grafts fits with a macrophage identification since the collagen-GAG grafts undergo rapid degradation during the T cell assay time frame. Type 3 cells had the most consistent location and staining morphology of all cell types, appearing in both test and control sections of most graft types. This reinforces

the hypothesis that type 3 staining morphology corresponds to a distinct cell type. Type 3 cells apparently possess abundant Fc receptors given the strength of their stain using only the secondary, non-specific antibody (control sections). The strong staining observed when anti-T cell antibody is eliminated from the staining procedure is further evidence that these are not T cells.

Type 4 cells were cells which conformed to the expected morphology of T lymphocytes: a round nucleus surrounded by a thin border of stained cytoplasm. The fact that these cells were observed only in grafts which showed signs of rejection strengthens this identification. The observation of these cells within blood vessels of rejecting grafts is further evidence that type 4 cells are T lymphocytes, since T cells are carried in the blood stream.

Because the T cell assay stains various cell types in addition to T cells, the sensitivity of the assay is questionable. It was for this reason that a negative control section, without the T cell antibody, was prepared for each biopsy assayed. Subtraction of this background signal was intended to reduce non-specific effects. The T cell assay was based on the assumption that subtracting the non-specific staining response (macrophages and generic lymphocytes such as PMNL's) would yield a signal which was a meaningful indicator of rejection.

The results obtained support this hypothesis. Control sections contained few stained cells relative to test sections, indicating that non-specific staining was not overwhelming a specific signal. Grafts known from previous studies to produce rejection showed a strong signal; those known to provoke no rejection showed a relatively weak signal. Also in excellent agreement is the fact that the statistical tests of significance used to analyze the raw data described in the Results indicated no significant difference between T cell level in unrejected grafts and intact skin. This was found despite the fact that many more stained cells were seen in grafts of any kind as compared to the intact skin. Subtracting the nonspecific stain value reduced the measured signal to a level that was not different from normal tissue.

(b) **Statistical analysis of data.** Examining the results of significance testing in detail can indicate whether the conclusions drawn from the significance testing are relatively strong or weak. The methods applied and results obtained in this study are considered below.

(c) **Methods.** Two criteria needed to be met before applying a common statistical method, the t test. The first is that the individual data points used to calculate a mean value for a certain response must fit a normal distribution. The Kolmogorov-Smirnov test was used to determine the significance of fit of the separate biopsy data points for each graft type to a normal distribution. The data for all graft types fit with 100% significance. The second criterion for using the t test is that the standard deviations associated with the data points for each response must not differ greatly. The Two-Sample Analysis function of the Statgraphics program supplied an answer to this question. Given two data sets and a chosen confidence level, this function provides a confidence interval for the ratio of the variances (standard deviation equals the square root of the variance). If the confidence interval includes 1, then the variances cannot be considered significantly different. A confidence level of 95% was chosen, and at this level all the standard deviations for the compared

data sets were not statistically different with the exception of comparing allocell ECM analogs and autocell ECM analogs.

Finally, an analysis was made of the significance of the sample size for each pair of data sets compared. The Normal Means function of the Statgraphics program was used for this purpose. An alpha value of 0.05 was chosen to characterize the likelihood of rejecting the hypothesis that the data sets are the same when in fact they are different. A beta value of 0.10 was chosen to characterize the likelihood of accepting the hypothesis that the data sets are the same when in fact they are different. The minimum number of observations needed to say that the data sets are different, i.e. to reject the hypothesis that they are the statistically the same, is given as output by this function. The results of this analysis indicated that a sufficient number of animals had been biopsied in each data set in order to perform statistically significant comparisons between the data sets. In cases where the *t* test indicated a significant difference between two data sets, the Normal Means function gave a minimum sample size that was less than the number of samples actually taken to conclude that there was a difference. Likewise, when the *t* test indicated no significant difference, the Normal Means function gave a large minimum sample size, indicating that it would be relatively difficult (requiring many samples) to prove that there was a significant difference.

(d) **Results of statistical analyses.** The Normal Means analysis of sample size significance generally strengthened the conclusions obtained by significance testing using the *t* test and Two-Sample Unequal Variance test. Most importantly, it verified that enough grafts had been biopsied to draw statistically significant conclusions from this study. However, it is worth noting the significant range of minimum sample sizes found for the various graft comparisons. The Normal Means analysis finds its greatest power when very large or very small minimum sample sizes are calculated. If the analysis says that only one or two samples are needed to conclude that the compared data sets are different, then this is a very strong result: the data sets are almost certainly different. If hundreds of samples are needed to say that the data sets are different, then it is quite likely that they are not different.

By this reasoning, most of the results obtained are strong. For example, only one sample is needed to be able to confidently conclude that silicone alone provokes a significantly greater response than ECM analog. Conversely, six hundred-fourteen samples would be needed to be able to confidently conclude that the autocell ECM analog response differs significantly from the autograft response.

Intermediate values calculated for the minimum sample size may be an indication that strong conclusions cannot be drawn from the given data comparison. Comparisons between allocell ECM analogs and autocell ECM analogs gave minimum sample sizes of fifteen. Therefore, even though 95% confidence level testing by the Statgraphics Two-Sample Unequal Variance method indicated no significant difference for this data set pair, the result is somewhat suspicious. This is compatible with other data that indicate differences in the response to these grafts. The wound healing response for allocell ECM analogs is qualitatively similar to that seen for autocell ECM analogs, but the neoepidermis formed with the former seems to be less stable and less new tissue is regenerated. In addition, type 4 putative T cells were seen in the allocell ECM analogs but not in the autocell ECM analogs, indicating a

greater immune response to the allocell ECM analogs.

7.5.2 Qualitative Results

(a) **T cell staining**. The T cell study produced a great deal of qualitative information in addition to quantitative measurements. The stained cell distribution results presented in the Results are too preliminary to stand on their own as interpretable data. These results are presented only as preliminary data which may be useful in other studies.

(b) **Wound healing**. The wound healing data presented in the Results are qualitative in nature. They can be summarized as follows:

The wound healing observations of the strain 2/strain 13 rejection model confirm that this is a valid model. Interstrain grafts are rejected and intrastrain grafts are accepted. Gross observations also suggest that these animals show a response to open wounds and cell-seeded ECM analogs which is comparable to that seen on the previously studied Hartley model. Therefore, new tissue synthesis in these strains, using the ECM analog technology, can be compared to previous studies.

The cell-seeded ECM analog was found to produce three different effects. The seeded cells sometimes proliferate to form a new epidermis, while on other occasions no proliferation was evident. Proliferation happened about 10% of the time in this study and at a much higher rate in Orgill's work [40]. The difference can probably be attributed primarily to speed of cell-preparation. Orgill's work [40] involved a team to prepare the cell-seeded grafts, while the graft preparation reported here was often done solo by the author. The solo technique takes considerably longer (a factor of 2 or 3 at least) and this longer *ex vivo* time for the cells is probably detrimental. Despite this inconsistency in seeded cell proliferation, some deviation from linear scar formation was usually seen. The final result of a non-proliferative graft can be the same as that of a proliferative graft. Significant wound expansion and new tissue synthesis is possible in each case.

This observation strengthens the possibility of using allocell ECM analogs in a skin replacement therapy. In general, it appeared from gross and histological data that the newly synthesized epidermis in these grafts was less stable than that seen in autocell ECM analogs. This might suggest a lack of utility for the allocell ECM analog technique. However, unstable autocell ECM analog epidermal tissue can occur on grafts that eventually synthesize abundant new tissue. In addition, new dermal tissue was seen in some long term allocell ECM grafts (two out of four). Clearly, more long-term grafts need to be studied, but these results indicate a clinical potential for the allocell ECM technique.

Finally, the observation that only two of the fourteen allocell ECM analog grafts studied here showed any gross signs of rejection also suggests that the allocell ECM analog might find clinical use.

7.6 Conclusions

An analog of extracellular matrix has been used as a carrier of foreign epidermal cells in transplantation experiments. Using a demonstrated rejection model and staining technique,

cells involved in graft rejection were quantified. Transplantation of epidermal cells produces a significantly ($p = 0.05$) lower response than transplantation of whole skin. This indicates that skin immunogenicity resides primarily in the dermis.

The transplantation of epidermal cells using the extacellular matrix analog showed no evidence of rejection in twelve out of fourteen grafts. In addition, long term (102 days) observations showed gross and histological evidence of synthesis of new dermis and epidermis. This indicates potential clinical use for allocell ECM analogs. Such grafts would avoid problems of autologous tissue availability.

Conclusions and Recommendations

1. Studies of dermal generation in the guinea pig were conducted by using analogs of extracellular matrix (ECM) as grafts on full-thickness skin wounds. ECM analogs were studied either as grafts that has been previously seeded with epidermal cells from various sources or as unseeded grafts.

2. A novel relation was observed between the ability of an ECM analog to delay the onset of wound contraction and aspects of chemical and physical structure (degradation rate, average pore diameter).

3. Cells migrating into ECM analogs were shown ultrastructurally to enter into very intimate relation with the surface of the ECM analog.

4. A light microscopic study based on the use of monoclonal mouse antibody against α-smooth muscle actin led to the suggestion that ECM analogs interfere with wound contraction either by interrupting the continuity of the myofibroblast network in the wound bed or by inducing cancellation of mechanical forces exerted by small clusters of such cells (through disorientation).

5. A laser light scattering procedure was developed which can be used to report quantitatively the extent to which newly synthesized dermis (by use of ECM analogs) is scar or a faithful replica of physiologic mature dermis or a tissue of intermediate character.

6. A method for separating Langerhans cell populations from a mixed dermal and epidermal cell population was studied in a preliminary way. Further progress along this direction requires substantial modification of the experimental method.

7. Cryopreservation of epidermal cells was demonstrated at $-196°C$ as well as at $-80°C$, using dimethylsulfoxide and glycerol as cryoprotectants.

8. An ECM analog seeded with epidermal cells from various sources was used to locate the source of significant antigenicity in full-thickness allografts. A model of clinical rejection was developed using inbred strain 2 and strain 13 guinea pigs, and a quantitative assay for rejection of grafts was developed using a monoclonal antibody specific for cells involved in rejection (T cells). The results suggest that dermal components, rather than epidermal cells are the primary targets of rejection.

9. The results of the transplantation study suggest a clinical role for the use of ECM analogs seeded with foreign cells.

10. It is recommended that further study be conducted of the only procedure known today which reproducibly induces regeneration of a nearly physiologic dermis and a physiologic epidermis in adult mammals. If sufficiently understood at the molecular level this procedure could become the definitive method for treatment of patients with burns.

11. Specifically, it is recommended that an *in vitro* model consisting of fibroblast-populated ECM analogs be used to study the effects of carefully controlled extracellular matrix environments upon fibroblast behavior. In this proposed study the relationship between ECM receptors (integrins), fibroblast activity (migration vs. wound contraction) and

collagen topography (loose fibrils vs. densely packed collagen surfaces) will be established. Changes in integrin receptor distribution, as determined by immunolocalization before and after the onset of contraction and regeneration, will be compared. Immunoelectron microscopy will be used to co-localize specific integrin receptors to α-smooth muscle actin crytoskeletal elements of contractile fibroblasts. These studies will determine whether porous ECM analogs influence the utilization and distribution of receptors used by fibroblasts either for contraction or for regeneration.

References

[1] Hay, E. D., *Mod. Cell Biol.* **2**:509–548 (1983).

[2] Loomis, W. F. *Developmental Biology* (Macmillan, New York) pp. 116–124 (1986).

[3] Smith, L. T., Holbrook, K. A. & Byers, P. H. *J. Invest. Dermatol.* **79**:93s–104s (1982).

[4] Blanck, C. E., & Hitchcock, K. R. *J. Cell Bio.* **105**:139 (abstr) (1987).

[5] Nimni, M. E. *Semin. Arthritis Rheum.* **13**:1–86 (1983).

[6] Billingham, R. E. & Medawar, P. B. *J. Exp. Biol.* **28**:385–402 (1955).

[7] Billingham, R. E. & Medawar, P. B. em J. Anat. **89**:114–123 (1955).

[8] Yannas, I. V., Burke, J. F., Huang, C. & Gordon, P. L. *Polym. Prepr. Am. Chem. Soc. Div. Polym. Chem.* **16**:209–214 (1975).

[9] Yannas I. V. in *The Surgical Wound*, en. Dineen, P. (Lea & Febiger, New York), pp. 171–190 (1981).

[10] Yannas, I. V., Burke, J. F., Orgill, D. P. & Skrabut, E. M. *Science* **215**:174–176 (1982).

[11] Yannas, I. V., Orgill, D. P., Skrabut, E. M. & Burke. J. F. in *Polymeric Materials and Artificial Organs*, ed. Gebelein, C. G. (Am. Chem. Soc., Washington, DC) pp. 191–197 (1984).

[12] Yannas, I. V., Burke, J. F., Gordon, P. L., Huang, C. & Ruberstein, R. H. *J. Biomed. Mater. Res.* **14**:511–528 (1980).

[13] Dagalakis, N., Flink, J., Stasikelis, P., Burke, J. F. & Yannas, I. V. *J. Biomed. Mater. Res.* **14**:511-528 (1980).

[14] Yannas, I. V. & Tobolsky, A. V. *Nature(London)* **215**:509–510 (1967).

[15] Yannas, I. V. *Rev. Macromol. Chem.* **C7**:49–104 (1972).

[16] Yannas, I. V., Burke, J. F., Huang, C. & Gordon, P. L. *J. Biomed. Mater. Res.* **9**:623–628 (1975).

[17] Dickinson, R. G. & Jacobsen, N. W. *Chem. Commun.* pp. 1719–1720 (1970).

[18] Sylvester, M.F., Yannas, I.V., Salzman, E.W. & Forbes, M.G. *Thromb. Res.* **55**:135–148 (1989).

[19] Gordon, P.L., Huang, C., Lord, R.C. & Yannas, I.V., *Macromolecules* **7**:954–956 (1974).

[20] Mandl, I., Maclennan, J.D. & Howes, E.L. *J. Clin Invest.* **32**:1323 (1953).

[21] Medawar, P.B. *Nature (London)* **148**:783 (1941).

[22] Regnier, M., Delescluse, C. & Prunieras, M. *Acta Derm Veneriol.* **53**:241–247 (1973).

[23] Bourin, M.C., Delescluse, C., Furstenberger, G., Marks, F., Schweizer, J., Klein-Zanto, A.J.P. &Prunieras, M. *Carcinogenesis (London)* **3**:671–676 (1982).

[24] Ferdman, A. & Yannas, I.V. *Trans. Soc. Biomater.* **10**:207 (1987).

[25] Grillo, H.C., Watts, G.T. & Gross, J. *Ann. Surg.* **148**:145–152 (1958).

[26] Yannas, I.V. in *Collagen: Biochemistry, Biotechnology and Molecular Biology*, ed. Nimni, M.E. (CRC, Boca Raton, FL), Vol. 3, pp. 87–115 (1988).

[27] Troxel, K. and Yannas, I.V., unpublished data.

[28] Gabbiani, G., Rayan, G.B. & Majno, G. *Experientia* **27**:549–550 (1971).

[29] Yannas I.V. in *Cutaneous Development, Aging and Reparid*, eds. Abatangelo, G. & Davidson, J.M. (Liviana Press, Padova, Italy) pp.131–139 (1989).

[30] Yannas, I.V., Lee, E., Skrabut, E.M., Orgill, D.P. & Murphy, G.F. *J. Cell Biol.* **105**:223 (abstr) (1987).

[31] Burke, J.F., Yannas, I.V., Quinby, W.C., Jr., Bondoc, C.C. & Jung, W.K. *Ann. Surg.* **194**:413–428 (1981).

[32] Heimbach, D., Luterman, A., Burke, J., Cram, A., Herndon, D., Hunt, J., Jordan, M., McManus, W., Solem, L., Warden, G. & Zawacki, B. *Ann. Surg.* **208**:313–320 (1988).

[33] Yannas, I.V., Krarup, C., Chang, A., Norregaard, T.V., Zervas, N.T. & Sethi, R. *Soc. Neuroci. Abstr.* **13**:1043 (1987).

[34] Yannas, I.V., Lee, E., Orgill, D.P., Skrabut, E.M., and Murphy, G.F. *Proc. Natl. Acad. Sci. USA* **86**:933-937 (1989).

[35] Kessel, R.G. and Kardon, R.H. *Tissues and Organs: A Text-Atlas of Scanning Electron Microscopy*, W.H. Freeman and Company, San Francisco (1979).

[36] Van de Hulst, H.C. *Light Scattering by Small Particles*, John Wiley and Sons, New York (1957).

[37] Yannas, I.V. and Burke, J.F. *J. Biomed. Mater. Res.* **14**:65-68 (1980).

[38] Eldad, A., Burt, A., Clarke, J.A. *Burns* **13(3)**:173-180 (1987).

[39] Murphy, G.F., Orgill, D.P., and Yannas, I.V. *Lab. Invest.* **63**:305-313 (1990).

[40] Orgill, D.P. "The Effects of an Artificial Skin on Scarring and Contraction in Open Wounds"Ph.D. Thesis, Harvard-MIT Division of Health Sciences and Technology, MIT (1983).

[41] Roitts, I.M. *Essential Immunology* 6th ed., Blackwell Scientific Publications (1988).

[42] Taylor, C.R. *Arch. Path. Lab. Med.* **102**:113 (1978).

[43] di Fiore, M.S.H. *Atlas of Normal Histology*, 6th ed., Eroschenko, V.P. ed., Lea & Febiger (1989).

[44] Clark, R.A.F. in *The Molecular and Cellular Biology of Wound Repair*, Clark, R.A.F. and Henson, P.M. eds. Plenum Press (1988).

[45] Naritokou, W.C. and Taylor, C.R. *J. Histochem. Cytochem.* **30**:253 (1982).